Bacterial colonization of low-wettable surfaces is driven by culture conditions and topography

*Adeline Marguier, Nicolas Poulin, Charline Soraru, Laurent Vonna, Samar Hajjar-Garreau, Philippe Kunemann, Aissam Airoudj, Grégory Mertz, Julien Bardon, Maxime Delmée, Vincent Roucoules, David Ruch, Lydie Ploux**

Dr. L. Ploux

Biomaterial and Bioengineering, U1121 Université de Strasbourg/INSERM, 11 rue Humann, 67000 Strasbourg, France

CNRS, 23 rue du Loess, 67000 Strasbourg, France

ploux@unistra.fr

Dr. A. Marguier, C. Soraru, Dr. L. Vonna, Dr. S. Hajjar-Garreau, Dr. P. Kunemann, Dr. A. Airoudj, Prof. V. Roucoules

Institut de Science des Matériaux de Mulhouse (IS2M), UMR7361 Université de Haute Alsace/CNRS, 15 rue Jean Starcky, 68057 Mulhouse, France

Université de Strasbourg, France

Dr. N. Poulin

Centre de Statistique de Strasbourg (CeStatS), Institut de Recherche Mathématique Avancée (IRMA), UMR750 Université de Strasbourg/CNRS, 7 rue René Descartes, 67084 Strasbourg, France

Dr. G. Mertz, Dr. J. Bardon, Dr. M. Delmée, Dr. D. Ruch

Luxembourg Institute of Science and Technology (LIST), 4362 Esch-sur-Alzette, Luxembourg

Abstract

Effect of surface low-wettability on bacterial colonization has become a prominent subject for the development of antibacterial coatings. However, bacteria's fate on such surfaces immersed in liquid as well as causal factors are poorly understood. We address this question by using a range of coatings with increasing hydrophobicity, to superhydrophobic, obtained by an atmospheric plasma polymer method allowing series production. Chemistry, wettability and topography are thoroughly described, as well as bacterial colonization by *in situ* live imaging up to 24h culture time in different liquid media. In the extreme case of superhydrophobic coating, substrates are significantly less colonized in biomolecules-poor liquids and for short-term culture only. Complex statistical analysis demonstrates that bacterial colonization on these low-wettable substrates is predominantly controlled by the culture conditions and only secondary by topographic coating's properties (variation in surface structuration with almost constant mean height). Wettability is less responsible for bacterial colonization reduction in these conditions, but allows the coatings to preserve colonization-prevention properties in nutritive media when topography is masked by fouling. Even after long-term culture in rich medium, many large places of the superhydrophobic coating are completely free of bacteria in relation to their capacity to preserve air trapping.

Keywords

Superhydrophobicity, biointerface with bacteria, culture conditions, surface properties, GLMM

1. Introduction

Bacteria can adhere on all surfaces to eventually form a biofilm.[1] This capacity triggers a serious threat to public health especially when biofilms grow on surfaces of medical devices or food industry materials.[2-6] The initial events of biofilm formation include bacterial attachment to surface. This attachment depends on the environmental conditions (bacterial species, medium, temperature, etc) and on the material surface properties. Chemical composition, topography, mechanical properties as well as wettability (hydrophobicity and hydrophilicity), surface energy and charge are the surface-related factors known to influence bacterial adhesion and biofilm development.[7-8] Some of them are specially examined for their great potential to create antibiofilm surfaces.[9]

Surface energy is one of the factors involved in bacterial attachment.[10-13] More particularly, low-wettable especially superhydrophobic surfaces demonstrated some promising potential to reduce surface colonisation by bacteria.[14-19] This prevention may be the result of reduced protein adsorption and entrapped air layer between the bacterial suspension and the surface[14, 20-22] However, contradictory results are reported.[23-24] Aside from high differences in nature and wettability of the surfaces used in these studies, a serious reason is the common confusion regarding the distinction between bacterial retention and adhesion. Indeed, in most cases, the methodology used to quantify bacteria on the surface needs to transfer, thus to remove, it from the liquid bacterial suspension for subsequent sample preparation (e.g. fixation, staining, drying, detachment) and observation (electronic or fluorescence microscopy, colony forming units –CFU- enumeration). Depending on wettability of the surface, bacteria can be picked up by the water-air interface and released from the surface as also demonstrated for bacteria and colloids[25-26]. Hence, only a fraction of the adhered population is retained on the surface, which especially depends on the wettability of the surface. Focusing on bacterial retention, recent studies have confirmed the high interest of superhydrophobic and omniphobic surfaces as self-cleaning surfaces and provided important insights about their mechanisms[27-28]. However,

studies fail to actually report results about bacterial adhesion and its mechanisms on such surfaces in a liquid environment. Understanding the mechanisms especially raises the important question of whether the material factors affect bacterial adhesion on low-wettable and superhydrophobic surfaces in liquid. Indeed, as noted by Busscher's group[29], "bacterial adhesion is governed by interplay of different physico-chemical properties". Thus, chemistry and topography are likely to influence bacterial adhesion on the surfaces by themselves, and independently from the resulting property of wettability and air entrapment. Even hydrophobicity of the bacterial cell wall has been shown to impact bacterial deposition and adhesion to surfaces[10, 30] sometimes as a combination with surface roughness[29]. Hence, the influence of surface hydrophobicity on bacteria deposition, adhesion and even mobility[31] has been widely investigated and multiple regression analysis have been used to attempt to distinguish the role of the different parameters. However, to the best of the authors knowledge, these effects have never been considered for low-wettable surfaces, especially regarding their implication for the actual bacterial adhesion in liquid. In addition, properly investigating this question imposes to describe such complex surfaces more accurately than in the published studies. Indeed, the wettability properties are usually only considered through static water contact angles (WCA) measurements, which is insufficient to investigate air trapping and anchoring of the liquid.[32-34] The surface chemical composition is also often only briefly described, and topography is rarely depicted beyond the common area roughness parameters Sa / Ra (arithmetical mean height) and Sq / Rq (Root mean square height) in 3D / 2D.[33-34] The two latter parameters only describe topography amplitude, and other parameters shall be provided if information related to the symmetry or spacing of topography has to be considered.[35] Thus, especially knowing the size of bacterial cells (from slightly less than to few microns) and their appendages such as pili and other fimbriae (diameter from few to several tens of nanometers), a more precise knowledge of the surface topography is essential.

Culture conditions (i.e. incubation time, bacterial culture medium, bacterial species) also impact bacterial adhesion and retention on surfaces[8]. Hence, they are prone to interact with the surface-related factors, thus enhancing, reducing or even hiding their effect. Due to high variation in culture conditions, this issue is made very difficult to be addressed on the basis of the published results. Combined with variations in regard to the methodology used to evaluate bacterial population adhered or retained on the surface, general conclusions about only the role of low wettability of a surface in the prevention of bacterial adhesion and development cannot be drawn for sure.

The aim of this paper is to determine whether low-wettable coatings immersed in a contaminating liquid are able to prevent bacterial adhesion and development in a durable way and to specify which factor(s) is(are) the most important in this control. The considered factors were the culture conditions (medium and time), the bacterial species and the chemical, topographic and wettability surface properties. The investigation was conducted on a range of coatings with increasing hydrophobic, to superhydrophobic, deposited by plasma polymerization as previously described.[36] The coatings are manufactured in high series by an adequate process easy to transfer to the industry. Surface properties were thoroughly investigated by X-ray photoelectron spectroscopy (XPS), atomic force microscopy (AFM) and dynamic water contact angle measurements. The microbiological experiments were conducted with a *Escherichia coli* (*E. coli*) K12 strain as a model, which is known to express curli and other pili[37]. The impact of the bacterial species especially regarding cell wall and shape was questioned by comparing colonization by *E. coli* with colonization by *Staphylococcus epidermidis* (*S. epidermidis*). Three different liquid surroundings, i.e. nutritive, rich (LB), nutritive, minimal (M63G), and no-nutritive (NaCl) media were considered which allowed us to investigate the possible influence of an adsorbed molecular layer on bacterial colonization of the hydrophobic/superhydrophobic surfaces. Importantly, bacteria were *in situ* analyzed on the

range of coatings by real-time fluorescence confocal microscopy under static or with low hydrodynamic conditions without any previous creation of air-liquid interface. Aside from ANOVA analysis used to determine statistical differences in the colonization between coatings, an innovative statistical analysis (general linear mixed models) allowed us to identify the precise surface properties exhibiting the greatest influence on bacterial colonization in given culture and environmental conditions.

2. Surface Characterization

2.1. Chemistry

The chemical properties of the coatings were investigated by XPS analysis. Binding energies corresponding to carbon (C1s), fluoride (F1s) and oxygen (O1s) were detected on XPS survey spectra for all the coatings, except for ppDOCA on which fluoride was not detected (**Table 1**). This is attributed to the presence of PFDA on all the coatings except on ppDOCA, since PFDA was the only possible source of fluoride on the surfaces. In addition, as shown by F1s peak, the amount of fluoride increased with the increase in polymerized PFDA. At the same time, the carbon amount decreased in relation to the decrease in DOCA content on the coating. The amount of oxygen (O1s) was almost constant due to similar number of oxygen atoms in the molecular structure of both PFDA and DOCA. In XPS high-resolution spectra of C1s, the binding energies were assigned to CHx/CC (285.28 eV), CO (286.96 eV), O=CO (289.07 eV), CFx-CF-CFx (288.74 eV), (-CF2) (291.35 eV) and CF2-CF3 (293.71 eV). Evolution of their amounts with the ratio of PFDA and DOCA amounts injected in the plasma chamber during the polymerization is described and discussed elsewhere.[36] It also allowed us to calculate the actual amount of PFDA (%PFDA) on the topmost surface of each coating as described in the Materials and Methods section. Based on the results, coatings were categorized into six classes of %PDFA (**Table 2**): 0% (ppPFDA0, i.e. ppDOCA); from 20% to 39% (ppPFDA20-39), from 40 to 59%

(ppPFDA40-59); from 60% to 79% (ppPFDA60-79); %PFDA from 80 to 99% (ppPFDA80-99); 100% (ppPFDA100, i.e. ppPFDA). Regarding reference surfaces, an expected high silicon (Si2p) signal was detected on SW while the oxygen peak (O1s) indicated the presence of an oxide layer as usually expected on silicon surfaces in contact with the atmosphere. Some organic contaminations, commonly occurring during the time between sample preparation and XPS analysis, were observed through the detection of a C1s peak. On PP, an expected high C1s signal was detected as well as a low O1s signal resulting from surface oxidation and traces of Si2p signal commonly used as charge in commercial PP.[38] Due to these changes in the surface composition, the surface charge may vary yet moderately from one surface to another. However, the ionic force of the three culture media used for microbiological studies is about 150 mM. This is high enough to expect that the surface charges are electrically screened due to the Debye length. Therefore, surface charges of bacteria and coatings' surfaces are not plausible factors of influence of bacteria adhesion in this study.

2.2. Topography

Surface topography was analyzed in terms of morphology (structure size, shape) and texture (structure density, sharpness) on 10 μm x 10 μm AFM images (0.78 Hz, 256 × 256 pixels). Topographic features possibly involved in the interface with bacterial cells were considered in addition to those usually accepted as sufficient to describe superhydrophobic surfaces and their interface with water and other liquids.[39] In particular, bacterial cells and the appendages they can possess (such curli and pili for the *E. coli* strain used in this study) may enter some concave features at the microscopic and nanoscopic scales (for bacterial cells and the appendages respectively). Hence, especially topographic parameters describing the surface in terms of valleys, valleys-to-peak ratio and distance between these features are of high importance.

As expected, PP and SW reference surfaces were both much smoother than all the coatings. According to AFM (examples in **Figure 1**), ppPFDA0 coating (i.e. ppDOCA) was also smooth and PFDA-containing coatings revealed heterogeneous globular grain structures. Density, width and height of the grains differed from one content in PFDA to another. Overall, grain size decreased with the increase of %PFDA from ppPFDA20-49 to ppPFDA60-79, while grains of small and high sizes coexisted on ppPFDA and ppPFDA80-99. The amplitude and spatial characteristics of this surface topography was precisely described by 14 parameters (**Table 2**). The most relevant are graphically depicted in **Figure S1.** Average roughness (Sa), root mean Square (Sq) and peak-peak height (Sz) were affected by the quantity of PFDA without being directly correlated to it (**Table 3** and **Figure S2**). For example, Sa varied from 44 ± 29 nm to 139 ± 8 nm with a maximum value on ppPFDA40-59 (146 ± 14 nm). In general, Sz showed peak-peak heights from 1 to 2 µm which is similar in size as bacteria and may therefore favor the retention of bacterial cells.[40-41] Moreover, surface skewness (Ssk) was positive for all the coatings with non-zero PFDA content (**Table 3**), which reveals that the topography is made of high convex but shallow concave structures.[42] This is supported by Spk/Svk higher than 1, which shows that height of the convex structures was usually greater than depth of the concave structures.[42] Thus, all the coatings except ppPFDA0 had micrometric structures with prevalence of convex structures of height higher than depth of the concave structures. Furthermore, the structures were in general narrow and sharp as demonstrated by the kurtosis surface (Sku) that was greater than or equal to 3 for all the coatings.[35, 42] Mean summit curvature (Ssc) shows that the radius of curvature of the convex structure sides even decreased with %PFDA. In addition, density of summits per μm^2 (Sds) increased with %PFDA from 2 ± 1 and 9 ± 1 convex structures /μm^2. These texture aspects were confirmed by the surface developed ratio (Sdr) which shows that coatings with the highest Ssc and Sds have also the highest value of Sdr, meaning more complex topography. In brief, texture analysis revealed that PFDA/DOCA coatings carried a

prevalence of convex structures of peak type, these structures being denser and sharper as the percentage of PFDA increases.

2.3. Wettability

Adding PFDA in the DOCA solution injected through the plasma discharge was expected to provide a range of coating wettability from hydrophobic to superhydrophobic. Advancing (θ_A) and receding (θ_R) water contact angle measurements showed in **Figure 2A** highlights two wetting regimes. The first regime was observed for %PFDA from 0% to79%. θ_A and θ_R increased with PFDA amount (from 87 ± 2° to 137 ± 4° and from 31 ± 7° to 42 ± 3° respectively) thus leading to the increase of contact angle hysteresis ($\Delta\theta$) (from 56 ± 3° to 105 ± 6°). This is characteristic for hydrophobic surfaces in Wenzel state, i.e. revealing intimate wetting by water. High hysteresis results from impaling of the water droplet in the structures of the rough surface.[43] In addition, increases of θ_A and of static contact angle θ^*, which are also observed on these surfaces, are due to increase of the contact area between our surface and droplet rather than less affinity with water.[43-44] The second regime was observed for coatings with %PFDA from 80% to 100% (**Figure 2B**): They all revealed higher θ_A value (155 ± 3°) and a noticeable increase in θ_R (102 ± 3° for 80-89% and 146 ± 4° for 100% PFDA) leading to the strong reduction of the hysteresis (up to 8 ± 4° for 100% PFDA). This characterizes trapping of air layer which prevents droplet attachment on the surface and is a common characteristics of the Cassie-Baxter state.[45] Nevertheless, the hysteresis values on coating with %PFDA from 80% to 95% (from 40 ± 5° to 60 ± 2°) reveal an affinity between the liquid and the surface despite trapping of air. This is specific for surfaces in a mixed Wenzel and Cassie-Baxter state, which is commonly called "rose petal effect".[46-48] By still increasing PFDA content, $\Delta\theta$ value continues to decrease with a strong reduction for coatings with %PFDA higher than 95% (22 ± 1° for %PFDA of 95%). Hysteresis was particularly low for the coating with 100% PFDA (8 ±

3°) and associated to high θ_A value. This demonstrates remarkable air trapping or, in other words, an extreme decrease of the fraction of wet material (Fwet) and thus of droplet attachment. On this coating, θ_A and $\Delta\theta$ values are on the margin of the accepted definition of the superhydrophobic state known as "lotus effect" (150° and 5° respectively).[49-50] This is probably due to some rare yet present defects at the surface. Indeed, as usual for engineered surfaces, coatings were not defect free. In addition, the manufacturing process was chosen to favor the production of high series and an easy transfer to the industry, adequate for robust biological results and further applications of the coatings. The resulting nanostructuration led to an overall wetting property, including superhydrophobicity, that however may have failed at some rare locations due to the presence of peaks and valleys that exceeded the mean size and shape of the suitable surface texture. Such heterogeneities can lower wettability by creating anchorage points of the liquid on the surface. Nevertheless, complementary measurements by the drop impact (bouncing) method (**Figure S3**) and the Wilhelmy plate method (**Figure S4**) have shown that the capacity of the most hydrophobic surface (100% PFDA) to resist wetting is kept and significantly higher than of the 90% PFDA coating (water column of 13 mm and 10 mm on ppPFDA and ppPFDA90 respectively; θ_A/θ_R=162°/145° and 153°/52° on ppPFDA and ppPFDA90 respectively). These two complementary approaches to the sessile drop method display the specific hydrostatic and confinement conditions associated to a sample completely immersed in liquid.[51-52] Such a resistance to wetting describe the 100% PFDA (ppPFDA) surface as a superhydrophobic, with significant air trapping. Finally, the range of coatings is composed of hydrophobic surfaces in Wenzel state (without trapped air) (%PFDA up to 80%), superhydrophobic surfaces with a mixed Wenzel and Cassie-Baxter state (%PFDA from 80% to 95%) and superhydrophobic surface in Cassie-Baxter state (with trapped air gradient) (%PFDA of 100%). SW and PP reference surfaces were characterized as hydrophilic (θ^* = 39 ± 2°, $\Delta\theta$ = 10 ± 4°) and hydrophobic (θ^* = 109 ± 6°, $\Delta\theta$ = 88 ± 5°) respectively. The wetting

properties of the different classes of coating did not significantly differ in the three culture media (**Figure S5)**. In addition, surface tensions of the media were lowered by the addition of bacteria at a concentration of 5 10^6 CFU/mL, but without significant dependency on culture time and at a level low enough to support the maintenance of similar wetting properties of the coatings in the presence of bacteria.

3. Colonization by bacteria according to PFDA content

Bacterial colonization was *in situ* investigated on the immersed surfaces without any creation of surface-air interface during the washing process. This enables to consider that the thermodynamic equilibrium was maintained throughout the whole experimental process up to and including the microscopy analysis. In general, colonization by *E. coli* evolved inversely with %PFDA (**Figure 3**). In NaCl especially (**Figure 3A**), a purely mineral medium without any nutritive compound, a significant decrease of adhered bacteria's number was observed with increase of %PFDA after 1h of culture. After 3h and 24h of culture, aside from a significant and expected growth of the adhered population (about 2 and 4 times more respectively, compared to 1h on the PP and SW reference surfaces), the impact of %PFDA on colonization was shown to be strongly reduced even though significant differences were still observed. Indeed, reduction of bacterial colonization between ppPFDA20-39 and ppPFDA80-100 coatings reached 65% after 1h of culture, but was only 30% after 3h and 10% after 24h of culture. In addition, some places were completely free of bacteria on ppPFDA80-100 coatings whatever the culture time (11%, 9% and 8% of the micrographs for 1h, 3h and 24h respectively) while places free of bacteria were never detected on all the other coatings and the reference surfaces. In hydrodynamic flow conditions, the reduction of colonization after 3h culture was even enhanced on the most superhydrophobic coating (**Figure 4**). This inverse effect of %PFDA on bacteria's number is consistent with the wettability properties of the coatings since

bacterial adhesion is expected to be lower on coatings with presence of trapped air layer (Cassie-Baxter state), i.e. ppPFDA80-100, than with absence of trapped air layer (Wenzel state), i.e. PFDA20-79. Similarly, due to the less retention of trapped air on ppPFDA (i.e. ppPFDA100) compared to ppPFDA80-99, colonization of ppPFDA should be less than of ppPFDA80-99. Besides, bacterial populations on the coatings shifted with time toward less mobility for all %PFDA (**Figure 4** and **Figure S6B**) but the fraction of mobile bacteria was higher on ppPFDA100 up to at least 3h of culture (from 40% to 15% on ppPFDA20-39; from 70% to 35% on ppPFDA100). This suggests unstable coating-bacteria interfaces due to the presence of air trapping and rearrangement of the air layer. This has already been demonstrated on superhydrophobic surfaces under liquid turbulence conditions[53] and was here illustrated by areas with air bubbles visible to the naked eye on the most hydrophobic coatings (**Figure S7**). The instability of the interface resulting from trapping air is thus expected to have favored mobility of bacteria on the most hydrophobic coatings. The vast majority of the authors also attributed to trapped air layers the capacity of low-wettable surfaces to reduce bacterial retention on the surface.[14-17, 34, 54-55] However, bacteria are here *in situ* (i.e. during immersion) visualized, thus ensuring that bacterial adhesion rather than retention is analyzed. The positive relation between bacterial adhesion and wettability on immersed surfaces is therefore here demonstrated for the first time.

Adhesion of *E. coli* after 1h and colonization after longer culture time evolved differently with %PFDA according to the medium (**Figures 3A, 3D, 3F**). In general, the more complex the medium was, the less the %PFDA seems to influence i.e. to prevent bacterial colonization. In minimal and nutritive M63G medium, bacteria's number adhered after 1h and 3h of culture (about 3 times more after 3h compared to 1h of culture on the reference surfaces) roughly decreased with %PFDA increase (55% of reduction between ppPFDA20-39 and ppPFDA80-100 coatings after 1h, 35% after 3h) (**Figures 3A, 3B**). As in NaCl medium, some places were

completely free of bacteria on ppPFDA80-100 coatings whatever the culture time (7% and 5% of the micrographs for 1h and 3h), which was rare on all the other coatings and the reference surfaces. However, the differences were lower, even though significant, than in NaCl medium and only coatings with %PFDA higher than 80% revealed different level of bacterial colonization than the others after 1h and 3h of culture. In addition, bacteria formed thick and similar biofilms on all the ppPFDA coatings after 24h of culture (**data not shown**). In LB medium, all the coatings were similarly colonized by *E. coli* after 1h of culture whatever %PFDA in terms of bacteria' number (**Figures 3C**). Nevertheless, a large fraction of places was free of bacteria on ppPFDA60-100 (7% of the micrographs for 1h) in contrast to the other coatings and reference surfaces. Similar result was obtained regarding colonization of the coatings and the reference surfaces by *S. epidermidis* cells cultured in LB (**Figure S8**).

Bacterial growth in the suspension as well as on the surface was obviously affected by the richness in nutritive compound in the medium. Therefore, bacteria's numbers measured on the reference surfaces after 1h of culture in M63G and LB were about 3 and 4 times the number measured in NaCl respectively. For this reason, also, adhered bacteria grew more in LB than in M63G. In NaCl, the adhered population is expected not to grow due to the lack of nutritive compound but the previous pre-culture in a nutritive medium provided bacteria enough nutrient to moderately grow after adhesion on the surface. Culture medium and incubation time also influenced the relation between bacterial colonization and %PFDA. This is attributed to molecules, mainly organic (i.e. biomolecules), present in the liquid medium, that adsorbed on the surface after immersion into the liquid.[8] They were not only initial compounds of the medium but also probably resulted from the increasing metabolic waste produced by bacteria during the culture. Thus, the surface was fouled as shown by XPS analysis of PFDA/DOCA coatings previously immersed in the three different media. After 3h of immersion and washing

with water, some places revealed modification of the surface chemistry despite withdrawal of the coatings from the medium (**Figure S9**). This fouling led to a reduction of air trapping on ppPFDA80-100 coatings as demonstrated by the significant increase of hysteresis especially measured after immersion of ppPFDA100 in LB (**Table S1**). Contact area between these coatings and bacteria is expected to have increased accordingly, thus resulting in a partial or complete deletion of the colonization prevention observed before fouling. Interestingly, however, a large number of places remained free of bacteria on ppPFDA80-100 coatings even though the inverse effect of %PFDA on bacterial colonization disappeared by increasing culture time and fouling capacity of the medium (**Figures 3A3, 3B2, 3C1**). This suggests that coatings with high %PFDA prevented the fouling of some surface places, which is in agreement with other works that reported the capacity of superhydrophobic coatings to prevent formation of adsorbed biomolecule layers.[22] These places may therefore have kept their initial capacity to resist wetting and consequent bacterial colonization even in long term cultures and in rich medium.

Aside from a direct effect of the surface wettability on the bacterial adhesion on immersed coatings, the inverse relation between %PFDA and bacteria's number demonstrated by these results may reveal the impact of other surface properties on bacterial adhesion. Regarding surface chemistry, numerous studies have shown reduction of bacteria's number on coatings with high content of CF_2 or CF_3.[6, 10, 16, 56-58] The effect is usually attributed to the absence of acid-base interactions between bacteria and the surface due to the electronegativity character of fluorinated groups.[6, 59-60] Furthermore, both morphology and density of the topographical structures present on the coatings may be a cause of reduction of bacterial colonization on ppPFDA80-100 in comparison with ppPFDA20-79. Indeed, convex structures were in higher density on coatings with higher PFDA content (8-9 structures/μm^2 on ppPFDA80-100 while 2-5 structures/μm^2 on ppPFDA20-79). This created structure-to-structure distances from 200 to

500 nm on ppPFDA20-79 corresponding to frequent areas with size like bacteria between the convex structures. In contrast, the distance between structures was smaller than 200 nm on ppPFDA80-100, resulting in surfaces almost free of such areas. This may be a reason why bacterial colonization was promoted on ppPFDA20-79 compared to on ppPFDA80-100 coatings since areas with bacterial dimensions have been shown to favor bacterial retention and thus colonization.[35, 40-41, 61] Furthermore, the contact area offered to bacteria by the sharp convex structures present on ppPFDA80-100 coatings was lower compared to the rounded structures of ppPFDA20-79. This factor was also reported to affect bacterial adhesion[62-63] and may be thus responsible to the reduction of the adhered bacteria's number observed on the coatings with high %PFDA compared to those with low %PFDA. It may have also favored the maintenance of mobility of a higher fraction of bacteria on coatings with high %PFDA.

4. Explanatory factors of coating's colonization by bacteria

To precisely identify the surface properties actually responsible for (in other words the most prone to explain) the inverse relation between %PFDA and bacteria's number and especially the colonization reduction observed on the less wettable coatings reported in the previous section, elaborate and detailed statistical analysis was needed. Seeking quantification of the load impact of each factor, we used a multivariate statistical analysis with consideration of all surface-related (parameters displayed in **Table 1**) and surroundings-related (medium, culture time) factors. Surface-related factors are the parameters displayed in **Table 1** and surroundings-related factors are medium and culture time. "Bacterial species" was also considered as a factor. For that purpose, results obtained with *S. epidermidis* in LB medium for 1h of culture were added to the results to be explained. Several steps were necessary to complete the analysis.

4.1. Hierarchical effect of species, medium, culture and surface-related factors

In a first step (***model^0***), all the possible factors of influence (i.e. explanatory variables) including bacterial species, medium, culture time and the material-related variables were considered. This was performed by the statistical GLMM model referred as *model^0*. Explanatory variables that were strongly interdependent were identified by using the VIFs, thus allowing us to only maintain non-redundant explanatory variables for the further step. Among 33 initial variables, 10 non-redundant explanatory variables were finally conserved by using this procedure (**Table S2**): O1s, $\underline{C}O$, O=$\underline{C}$-O, $\underline{C}F_x$, Sq, Ssk, Sdr, θ_A (advancing water contact angle) and $\Delta\theta$ (hysteresis) for the chemical, topographical and wettability properties of coatings; Species, Medium and Time for the culture conditions. Furthermore, two versions of *model^0* were applied to the so-selected non-redundant explanatory variables: One considered the explanatory variables and their interactions ("*with interactions*"); The other considered the explanatory variables alone ("*without interactions*"). According to their respective AIC values, *model^0 without interactions* (the lowest AIC value) was accepted as the most relevant of both (**Table S2**).[46] Its results are reported in **Table 4**. They show that variations of bacteria's number on the surfaces are significantly (p-value < 0.001) and mainly (LI absolute value > 7) explained by the culture conditions, i.e. medium, culture time and bacterial species. Decreasing ranking based on the absolute value of LI demonstrates that medium has the predominant impact on bacteria's number adhered on the surfaces (LI ~ 31), followed by culture time (LI ~ 16) and bacterial species (LI ~ 7). Additionally, surface-related variables are only displayed by $\underline{C}F_x$ which has significant (p-value < 0.001) but lower impact (LI ~ 3). Among the non-redundant surface-related variables, $\underline{C}F_x$ is the variable the most related to plasma surface treatment and its changes are linked to the other chemical, topographic and wettability changes of the surface. $\underline{C}F_x$ therefore probably characterizes the global impact of the coatings on surface colonization. The low absolute value of its LI is thus indicative of the very few influence of surface properties

compared to culture conditions. The trend was similar when investigation focuses on finding the most important explanatory factors for each individual medium and each specific bacterial species (***model[1]***) (**Table S2** for VIFs-based selection and AIC values). Culture time has then proven to be the most predominant factor of influence on adhered bacteria's number (LI ≥ 7), much higher than all the surface-related factors (LI < 2) (**Table 3**). This predominant influence of the culture conditions on bacterial adhesion is due for a part to the high difference in bacterial growth between non-nutritive, minimal and rich media. This is responsible for high changes in the adhered bacteria's number, which may screen more moderate influences such as those expected from changes in the surface properties. Furthermore, this probably displays the substantial variation of the surface biofouling by biomolecules coming from surroundings according to medium and culture time. In addition, bacterial adhesion may vary significantly with bacterial species,[10-11] which may thus overtake lower impacts of surface properties. Finally, this provides a quantitative and statistical justification of common methodological practices in bacterial adhesion and biofilm studies, in which minimal medium is favored in order to avoid any masking of the potential material-related effects.[64] The important role of other culture conditions such as static/dynamic/stirring have been also highlighted by other authors for superhydrophobic coatings specifically.[16-17, 24] From an application point of view, these results suggest that bacteria-preventive effects of superhydrophobic surfaces can only be expected under specific conditions of medium and duration of use. This may also explain contradictory results reported in the literature regarding bacteria-preventive performances.[34, 54]

4.2. Hierarchical effect of the surface-related factors

In a last step, we focused on the hierarchical effects of the factors specifically related to coating's surface properties. The statistical analysis (***model[2]***) was performed for each specific culture condition i.e. each specific medium, culture time and bacterial species. The non-

redundant explanatory variables selected based on VIFs and the AIC values needed for selecting the most relevant model version (i.e. with or without interactions) are reported in **Table S2**. According to AIC values the selected models were *model^2 with interactions* for *E. coli* in NaCl at 1h and 3h of culture, and *model^2 without interactions* for 24h of culture in NaCl medium, and for all culture times in M63G and LB media.

Their results, reported in **Table 4,** show that all the non-redundant explanatory variables had a significant impact for 1h and 3h of culture (p-value ≤ 0.001). According to their load impact, parameters that predominantly explain changes in bacterial colonization of PFDA/DOCA coatings concern topography, especially Ssk and Sdr by their own action or by the action of their interaction (for Ssk, Sdr and Sdr:Ssk respectively, LI ~ 110, 32 and 109 for 1h of culture and Li ~ 42, 21 and 88 for 3h of culture). The number of adhered bacteria decreases with the increase of Ssk (peak-to-valley predominance) and Sdr (density and sharpness of the peaks) values, which is indicated by the negative sign of the LI associated to these explanatory variables. This reveals an effect significantly higher than those of chemical and wettability parameters (LI < 10). Regarding chemistry, this result is consistent with those reported by several authors, which shown that chemistry is a factor of influence easily masked by others.[10, 65-66] Regarding air trapping, effect on bacterial adhesion may have been partially masked because it only varies for the narrow range of coatings with Cassie-Baxter state (%PFDA from 80% to 100%). In contrast, surface topography highly varies throughout the complete range of %PFDA. However, predominance of topography is high enough to be stated here. This strong effect is probably related to typical dimensions of the topographical structures at the coating surface. Indeed, made of globular peaks and valleys, the surface also provides flat places that are close to bacterial size (1 µm height, 0.5 µm diameter) on ppPFDA20-79 coatings but reduced under the size of one bacterial cell on ppPFDA80-100 coatings. ppPFDA20-79 coatings may thus retain bacteria by offering large contact areas and protection against shear

forces[35, 40, 61] while contact area becomes smaller and unfavorable to bacterial adhesion on ppPFDA80-100 coatings.[41, 62-63] ppPFDA80-100 coatings are also characterized by their ability to trap air, which lowers the space available for cell adhesion. This is consistent with the strong reduction of adhered bacteria's numbers observed with increase of Sdr that especially describes surface texture (**Table 4**). Accordingly, number of places on ppPFDA80-100 showed a notable resistance to colonization (**Figure 3**). Besides, the analysis reveals a significant and high impact (LI = 33) of the interaction between a wettability property (hysteresis, $\Delta\theta$) and Ssk at 1h of culture. This illustrates the strong role of topography (described by Ssk) in the surface ability to behave according to Cassie-Baxter model, i.e. to trap air in the valleys of the topography (described by $\Delta\theta$; LI = 8). Positive sign of the $\Delta\theta$:Ssk LI indicates that effect of $\Delta\theta$ reinforces the singular effect of Ssk. In other words, air trapping ability of the surface, which increases as $\Delta\theta$ enhances the effect created by peaks compared to the effect of topography alone.

After 3h of culture in NaCl medium, only factors related to topography significantly affected the number of adhered bacteria on the coatings, without any effect of $\Delta\theta$ (**Table 4**). After 24h of culture, even effect of topography factors, here displayed by Sq, was no longer significant. This reflects the decrease in air trapping and in contrary the increase in the fraction of wet material (Fwet) (as shown by hysteresis in **Table S1**). Indeed, weight forces were exerted on the liquid throughout culture time, thus causing the progressive wetting of the surface. In M63G and LB media, topography factors were shown not to affect bacterial adhesion as early as for 1h of culture. In addition, wettability (described by $\Delta\theta$) only revealed very slight (LI < 2) even though significant and positive effect (positive LI sign) on the adhered bacteria's number. The specific chemical composition of PFDA/DOCA coatings (here displayed by CFx) also slightly yet significantly affected bacterial adhesion (LI ~ 1) in M63G medium, negative sign of LI being consistent with reduction of adhered bacteria's numbers with increase of PFDA content. These results show that a low hysteresis is still beneficial to reduction of bacterial adhesion in

media with moderate or even high content of organic compounds such as M63G and LB media. However, effect is very weak probably due to formation of a conditioning film by adsorption of molecules coming from the medium. This may have led to filling of the surface structuration by adsorbed mass, thus harmonizing bacterial retention due to topography. Fouling could not be directly visualized by an experimental method but indirectly stated but XPS analysis as displayed in **Figure S9** and previously discussed. However, as displayed in **Figure S7,** some air bubbles remained visible to the naked eye on superhydrophobic coatings immersed in M63G and LB media. Such areas that have been demonstrated to illustrate the air trapping capability of superhydrophobic surfaces[67-68] covered from 5 to 30% of the ppPFDA80-99 and ppPFDA surfaces, while they were absent on the other coatings. As a result, they also remained almost free of bacteria (**Figure S7**), which is consistent to the existence of many bacteria-free places on ppPFDA80-100 even after long culture time in NaCl or cultures in M63G or LB (**Figure 3**). The dependence of the bacteria-free places with the air trapping capability of the superhydrophobic surfaces is shown by the significant impact of $\Delta\theta$ and CFx (both descriptors of the superhydrophobic coatings) on the number of adhered bacteria.

Finally, GLMM analysis shows that surface topographic properties influence bacterial colonization of nanostructured PFDA/DOCA coatings much more than wettability and chemical properties. In other words, chemistry and wettability appear not to be the essential factors in the reduction of bacterial colonization on hydrophobic/superhydrophobic surfaces such as those studied here. Nevertheless, superhydrophobic surfaces with Cassie-Baxter state are the most suitable to prevent bacterial colonization. They can associate sharp and dense nanotopography strongly unfavorable to bacterial retention with a lotus effect which remains active, even though weakly, when nanotopography is smoothed by an adsorbed layer of biomolecules. Results reported here thus show that $\Delta\theta$ is not a sufficient surface descriptor to predict bacterial retention and colonization on superhydrophobic surfaces. At least topographic-

related factors such as structure shape, size and density must be also taken into account. Besides, superhydrophobic coating's performances regarding bacteria colonization were shown to be enhanced under hydrodynamic flow conditions, probably as the result from the unstable coating-bacteria interface due to air trapping and rearrangement of the air layer.

Nanotopography and low-wettability may have both impacted bacterial colonization during deposition, contact, adhesion or further fouling. Indeed, bacterial colonization is a complex, kinetic process, which consists in a succession of events (cell transport to the surface, cell-to-surface contact, reversible and irreversible adhesion with possible, previous motility, cell proliferation for colony and biofilm formation) that can all be driven by physico-chemical aspects such as thermodynamic laws[69-71] and hydrodynamics[71-72]. However, evolution of these events with time (in other words, time boundaries between the events) highly depends on the culture conditions. This implies that results obtained at a specific time may correspond to a different phase of the process according to the culture conditions. Typically, confocal microscopy analysis indicated that proliferation did not start after 1h of culture in NaCl (only single cells) while observation at 1h occured during proliferation in LB (frequent couple of aligned cells) and M63G (rare couple of aligned cells). Nevertheless, precise time boundaries between transport and contact phases, contact and reversible adhesion phase, and reversible and irreversible adhesion phases are unknown, which prevents to more specifically relate the effect of nanotopography and low-wettability, and the corresponding thermodynamic aspects, to the phases that were especially impacted.

5. Conclusion

In this work we used a series of atmospheric pressure plasma polymer coatings exhibiting wetting properties ranging from hydrophobic to superhydrophobic, to study the role of this surface feature on bacterial adhesion and colonization. Our results demonstrate that

colonization is by far predominantly controlled by culture conditions such as medium composition, culture time and bacterial species rather than all surface properties considered in this study (chemistry, topography, wettability). To some extent, the presence of peak structures was shown to decrease bacterial adhesion and colonization when using a non-clogging medium. The effect of hydrophobicity, as measured by wettability, was finally low and only visible if topography was screened by fouling. The most hydrophobic coating, depicted as superhydrophobic, clearly detaches from the series of hydrophobic coatings. This coating was indeed shown to clearly reduce bacterial adhesion and colonization with areas completely free of bacteria whatever the surrounding media, even after static long time culture or under hydrodynamic flow conditions. Finally, low-wettability thus provides some low but significant prevention of colonization in all liquid surroundings including biomolecule-rich and for long term time of use. In contrast, changing density and size of the surface nanostructuration at a level of 100 nm average height reduces bacterial colonization more than changing wettability only in a non-clogging medium.

The topography, wettability and heterogeneity of the coatings are specific to the manufacturing method, here through an atmospheric plasma deposition process. By considering the interplay between both topography, wettability and culture conditions, our statistical approach provides however key insights for the design of low-wettable surfaces with bacterial anti-adhesive properties that might be obtained with other techniques.

6. Experimental Section

Surface preparation

Coatings: Coatings were synthesized from two monomers: Dodecyl acrylate (DOCA) (~90%) and 1H,1H,2H,2H-perfluorodecyl acrylate (PFDA) (97%) (Sigma, France). They were deposited on silicon wafers (1 cm × 1 cm) purchased from MCR (Germany) using an

atmospheric pressure dielectric barrier discharge (DBD) reactor described by Petersen *et al*..[73] More details about the method of depositing a series of coatings made from different concentrations of DOCA and PFDA precursors (monomers) is described by Mertz *et al*..[36] In short, a plasma polymer coating with a low level of precursor fragmentation is deposited from a mixture of DOCA and PFDA. The hydrophobic character of the coating increases with the ratio of PFDA in the precursor mixture, as well as its roughness amplitude and complexity, thereby providing a coating whose wettability is ranging from hydrophobic (pure DOCA) to superhydrophobic (pure PFDA).

Coatings are named in regard to the actual fluorine concentration in the coating as measured by XPS (see below). In addition, coatings are grouped in ranges of 20% in general. For instance, ppPFDA20-39 means a plasma polymer coating in which the percentage of PFDA (%PFDA) is comprised in the range from 20% to 39%. ppPFDA0 and ppPFDA100 are the coatings obtained from pure DOCA and pure PFDA respectively and are also named ppDOCA and ppPFDA respectively. For clarity reason, appellations such as ppPFDA20-79 are also used to replace the addition of several 20% ranges i.e. "ppPFDA20-39, ppPFDA40-59 and ppPFDA60-79" in this example.

Reference surfaces: Two reference surfaces were used. The first reference was silicon wafer (SW), purchased from Si-MAT (Germany), cut into pieces of 1 cm × 1 cm. They were cleaned by three successive baths with pure solution of chloroform (99%) under ultrasound for 15 min at 45 kHz (Transonic TI-HF, Elma) and at room temperature. Between baths, samples were rinsed with distilled water. The second reference was a commercial polypropylene surface (PP), purchased from Novaplest (France), cut into pieces of 1 cm × 1 cm. They were cleaned by three successive baths with pure solution of hexadecane (99%), chloroform (99%) and alcohol (70%) under ultrasound at 45 HZ for 15 min and at room temperature. Between baths, samples were

rinsed with distilled water. SW were sterilized by dry heat during 1h at 180°C and PP by UV-C exposure (λ = 254 nm) during 7 min at 150 mm distance from the lamp.

Surface characterization

Chemical composition by X-ray Photoelectron Spectroscopy (XPS): Topmost surface characterization was carried out by X-ray induced photoelectron spectroscopy (XPS) on a VG SCIENTA SES-2002 spectrometer equipped with an Al Kα monochromatic x-ray source (1486 eV) at a power of 420W (14 kV, 30 mA). XPS analysis was carried out under pressure of 10^{-9} mbar, on areas of about 4 mm × 6 mm and with scanning energy of 500 eV for general spectrum and 100 eV for high-resolution spectra of carbon (1s), oxygen (1s) and fluorine (1s). The binding energy of CHx / C-C groups (285.0 eV) was used as a reference. Peaks were deconvolved using CASA-XPS software into several components (**Table 1**) with symmetric function and energies were set on the basis of bibliography.[74] Quantity and atomic percentage of the elements were determined by measurement of the peak areas and considering transmission function of the spectrometer, cross section and free average course.[75]. Effective cross-section is 1.00 for C (1s), 4.43 for F (1s) and 2.93 for O (1s). The fraction of PFDA molecules among the components present at the extreme coating surface (%PFDA) was determined using the theoretical atomic ratios in the structure of each molecule as displayed in **Equation 1** (calculation detailed in **Figure S10**):

$$\%PFDA = A_{F1s} + 2 \times A_{CF2} + A_{CF3}. \quad \textbf{(1)}$$

Topographical feature by Atomic Force Microscope (AFM): AFM analysis of surface topography was performed in tapping mode using a Nanosurf FlexAFM Microscope with ACT tip (L: 125µm, W: 30µm, T: 4.0µm, f: 200-400Hz, k: 13-77N/m), scan rate of 0.78 Hz and resolution of 256 × 256 pixels. Before each acquisition, surfaces were cleaned under nitrogen stream. Experiments were done in air at room temperature. Three zones of 10 µm × 10 µm were

acquired per sample and AFM analysis was repeated on 3 samples of each surface type. AFM images were treated by SPIP^{TM} software (version 6, Image Metrology company). 14 parameters (**Table 2**) were calculated according to ISO 25178, which allows very precise description of the amplitude and spatial characteristics of the surface topography. A graphic definition of the parameters that were later shown as the most relevant ones is depicted in **Figure S1.** They are Surface Skewness (Ssk), Amplitude Surface Kurtosis (Sku), Reduced Height Ratio of Summit with Valley (Spk/Svk) and Surfaces Developed Area Ratio (Sdr).[42]

Wettability by water contact angle measurements: Surface wettability (i.e. hydrophilic, hydrophobic, superhydrophobic) and wettability states (Wenzel, Cassie-Baxter, Mixed) were determined by measuring static and dynamic water contact angles. Measurements have been done with a DSA 100 goniometer (KRUSS). A sessile water droplet of 4 µL was deposited on the surface via a needle which was made hydrophobic from a dedicated treatment (HY-Kit, Dataphysics). For advancing and receding contact angles, the droplet volume was gradually increased and decreased of 0.1 µL s^{-1}. Values of static, advancing and receding contact angles were extracted from the images captured by a CCD camera by using numerical fits of the droplet shape based on a Laplace-Young model. Water contact angle hysteresis was calculated as the difference between the advancing and receding water contact angles. Results are displayed as average and standard deviation of three measurements per sample.

Surface colonization by biomolecule

The samples were immersed during 3h at 30 °C, in 3 different culture media (NaCl, M63G, LB). After dewetting, the ratio between amounts of the PFDA and DOCA components on the coating (%PFDA) was determined by XPS analysis, according to the same technical specifications as described above. On each sample two different zones were analyzed: one with liquid retention and the other with complete dewetting.

Surface colonization by bacteria

Bacterial species and culture media: Bacterial experiments were conducted with two bacterial species. *Escherichia coli SCC1* (MG1655 with chromosomal insertion of $P_{A1/04/03/}$_*gfp*mut3*) (*E. coli*)[37] is a curli producing bacteria with a 1 µm height x 0.5 µm width rod shape.[76] *Staphylococcus epidermidis* RP62A (ATCC 35984) (*S. epidermidis*)[77] is described as a sphere ranging from 1 to 2 µm diameter and is a slime producing coagulase-negative-*staphylococcus*. *E. coli* MG1655 and *S. epidermidis* RP62A species have both hydrophilic bacterial cell wall.[59, 77-78] Three culture media have been used for this experiment: a nutritive, rich Lysogeny-broth medium (LB) (Sigma, France) that contains 10 g L^{-1} of tryptone, 5 g L^{-1} of NaCl, yeast extracts and vitamins; a nutritive, minimal M63G medium (pH 6.8) that contains 13.6 g L^{-1} of KH_2PO_4, 2 g L^{-1} of $(NH_4)_2SO_4$, 0.2 g L^{-1} of $MgSO_4$, 0.5 mL L^{-1} of 1% solution of FeS, 1 mL L^{-1} of 0.05% thiamine solution, 20 mL L^{-1} of 10% glucose solution and 11.8 mL L^{-1} of 6 M KOH solution;[79] a un-nutritive media (NaCl) that contains 9 g L^{-1} of NaCl.

−80°C frozen bacteria were incubated overnight on LB (Sigma, France) agar plate, at 30°C for *E. coli* and 37°C for *S. epidermidis*. Then, a liquid pre-culture was prepared with one colony of *E. coli* or *S. epidermidis* in LB medium and incubated for about 18h at 30°C and 37°C respectively. A culture was further prepared with 10% of pre-culture and incubated for 4h at 30°C for *E. coli* and 37°C for *S. epidermidis*. Bacteria were then harvested by centrifugation (3500 rpm, 4°C, 20 min). According to the experiment (see the next session), bacteria pellets were re-suspended in the medium of interest (LB, M63G or NaCl). Bacterial suspensions were adjusted to an absorbance at 600 nm (A600 nm) of 0.01 ($5\ 10^6$ CFU mL^{-1}).

Bacterial colonization assays: Coatings with various PFDA content (from 0 to 100%) and reference surfaces were immersed in 4 mL of bacterial suspension made in LB, M63G or NaCl according to the experiment. Before immersing, surfaces were fixed with glue (Aqua Silicone; Den Braven, Netherlands) on the bottom of Petri dishes to prevent them from floating. Samples were incubated for 1h, 3h and 24h at 30°C or 37°C for *E. coli* and *S. epidermidis*, respectively.

Coatings and reference surfaces were then thoroughly and carefully rinsed 8 times by replacing 1 mL of the bacterial suspension by 1 mL of fresh NaCl solution to remove non-attached bacteria. Particular attention was payed not to create surface-air interface for avoiding any displacement of adhered bacterial cells and maintaining the thermodynamic equilibrium conditions, thus focusing on bacterial adhesion rather than retention.[25] *S. epidermidis* adhered on the surfaces were fluorescently stained by adding 1 µL mL^{-1} of 5 10^{-3} M Syto9® (Invitrogen, US) stock solution and were incubated for 15 min. Then surfaces were directly observed in the last rinsing solution by using the fluorescence/reflection mode of an upright confocal microscope (LSM700 Carl ZEISS, Germany) equipped with a long working distance water objective (W Plan-Apochromat 63X/1.0, working distance 2.0 mm, Zeiss®). On each surface, micrographs were taken on 8 random locations. For each medium (LB, M63G or NaCl), experiments were conducted with two surfaces of each type and reproduced by 3 independent experiments. Confocal micrographs were analyzed by ImageJ V.1.44d software® (NIH).[80] Each image was processed to select the color channel and adjust thresholds by Otsu or Intermodes method depending on the intensity histogram of each image. Then, the number of adhered bacteria and their size on each micrograph were calculated with help of the analyze particle plug-in.

Bacterial colonization and mobility assays under hydrodynamic conditions: Coatings with typical PFDA content corresponding to hydrophobic, Wenzel and Cassie-Baxter behavior of the surface (ppPFDA20-39, ppPFDA80-99 and ppPFDA100 respectively) were placed in a home-made culture chamber **(Figure S6A)** connected to a real-time imaging setup described elsewhere[81] and dedicated to an up-right fluorescence confocal microscope (Zeiss LSM700). Measurements were performed over 3h of culture in NaCl 9g/L medium. The culture chamber was installed under a x63 objective and was perfused with fresh medium over the culture duration according to a procedure described elsewhere[82]. Bacteria were injected just after

acquisition was started and micrographs were taken every minute. Bacteria numbers were determined on micrographs as described in the previous section. They are presented as their average for periods of 15 min. Sub-populations of mobile and non-mobile bacteria in contact with the surfaces were determined by using ImageJ® and plugins. Bacteria with displacement longer than the bacterial length were defined as mobile.

Statistical analysis

In a first step, statistical analysis was performed on number of adhered bacteria as a function of PFDA surface content. ANOVA and Student's *t*-tests for equal variance for paired samples were performed to assess the statistical significance of our results. $\bar{x}$ is the average of bacteria number either adhered or mobile on the surface.

In a second step, general linear mixed models (GLMMs) were fitted to investigate links between the number of adhered bacteria ("variable to be explained") on coatings and reference surfaces with all the parameters and factors describing the experimental conditions and likely to change between experiments ("explanatory variables"). 33 parameters or factors were considered, which includes chemical and topographical properties, wettability, culture medium, bacterial species and incubation time. More precisely, to determine which explanatory variables or their interactions control bacterial colonization on the coatings, statistical models were run on the data frame of 3389 observations according to three levels: (i) the first model, named as "$model^0$" considers all the observations and explanatory variables, (ii) the second model, named as "$model^1$" considers only observations obtained for a specific medium and a specific bacterial species, (iii) the third model, named as "$model^2$" considers only observations obtained for a specific medium, a specific bacterial species and a specific incubation time. The number of the considered observations decreased therefore from $model^0$ to the $model^2$.

For each level, VIF (Variance Inflation Factor) statistical criteria was used to deal with collinearity among the explanatory variables. Then models including simple interaction among the explanatory variables were fitted. Selection of the best model, for each level, was made by backward selection with respect to the AIC (Akaike Information Criterion, the lower being the better). Likelyhood Ratio Tests (LRT's) were used to assess significance. All the statistical analyses were computed with R2.15® (GNU, public license).

Supporting Information

Supporting Information is available from the Wiley Online Library or from the author.

Acknowledgements

The present project was funded by the Centre National de la Recherche Scientifique (CNRS), the Luxembourg funding organization (Fonds National de la Recherche) through the HABaC project and the Alsace region (France). The authors thank Nayana Tusamda Wakhloo for having revised the English language.

References

[1] Donlan, R. M., *Emerg. Infect. Dis.* **2002,** *8* (9), 881-890.
[2] Carpentier, B.; Cerf, O., *J. Appl. Bacteriol.* **1993,** *75* (6), 499-511.
[3] Costerton, J. W.; Stewart, P. S.; Greenberg, E. P., *Science* **1999,** *284* (5418), 1318-1322.
[4] Wingender, J.; Flemming, H.-C., *Int. J. Hyg. Environ. Health* **2011,** *214* (6), 417-423.
[5] Katsikogianni, M.; Missirlis, Y. F., *Eur. Cell. Mater.* **2004,** *8*, 37-57.
[6] Ista, L. K.; Fan, H.; Baca, O.; López, G. P., *FEMS Microbiol. Lett.* **1996,** *142* (1), 59-63.
[7] Palmer, J.; Flint, S.; Brooks, J., *J. Ind. Microbiol. Biotechnol.* **2007,** *34* (9), 577-588.
[8] Ploux, L.; Ponche, A.; Anselme, K., *J. Adhes. Sci. Technol.* **2010,** *24*, 2165-2201.
[9] Glinel, K.; Thebault, P.; Humblot, V.; Pradier, C. M.; Jouenne, T., *Acta Biomater.* **2012,** *8* (5), 1670-1684.
[10] Bakker, D. P.; Huijs, F. M.; de Vries, J.; Klijnstra, J. W.; Busscher, H. J.; van der Mei, H. C., *Colloids and Surfaces B: Biointerfaces* **2003,** *32* (3), 179-190.

[11] Gottenbos, B.; Grijpma, D. W.; van der Mei, H. C.; Feijen, J.; Busscher, H. J., *J. Antimicrob. Chemother.* **2001,** *48*, 7-13.
[12] Nguyen, V. T.; Chia, T. W. R.; Turner, M. S.; Fegan, N.; Dykes, G. A., *J. Microbiol. Methods* **2011,** *86* (1), 89-96.
[13] Pratt-Terpstra, I. H.; Weerkamp, A. H.; Busscher, H. J., *Curr. Microbiol.* **1988,** *16* (6), 311-313.
[14] Crick, C. R.; Ismail, S.; Pratten, J.; Parkin, I. P., *Thin Solid Films* **2011,** *519* (11), 3722-3727.
[15] Poncin-Epaillard, F.; Herry, J. M.; Marmey, P.; Legeay, G.; Debarnot, D.; Bellon-Fontaine, M. N., *Materials Science and Engineering: C* **2013,** *33* (3), 1152-1161.
[16] Privett, B. J.; Youn, J.; Hong, S. A.; Lee, J.; Han, J.; Shin, J. H.; Schoenfisch, M. H., *Langmuir : the ACS journal of surfaces and colloids* **2011,** *27* (15), 9597-9601.
[17] Tang, P.; Zhang, W.; Wang, Y.; Zhang, B.; Wang, H.; Lin, C.; Zhang, L., *Journal of Nanomaterials* **2011,** *2011*, 8.
[18] Falde, E. J.; Yohe, S. T.; Colson, Y. L.; Grinstaff, M. W., *Biomaterials* **2016,** *104*, 87-103.
[19] Carman, M. L.; Estes, T. G.; Feinberg, A. W.; Schumacher, J. F.; Wilkerson, W.; Wilson, L. H.; Callow, M. E.; Callow, J. A.; Brennan, A. B., *Biofouling* **2006,** *22* (1), 11-21.
[20] Ellinas, K.; Kefallinou, D.; Stamatakis, K.; Gogolides, E.; Tserepi, A., *ACS Appl. Mater. Interfaces* **2017,** *9* (45), 39781-39789.
[21] Stallard, C. P.; McDonnell, K. A.; Onayemi, O. D.; O'Gara, J. P.; Dowling, D. P., *Biointerphases* **2012,** *7* (1), 31.
[22] Koc, Y.; de Mello, A. J.; McHale, G.; Newton, M. I.; Roach, P.; Shirtcliffe, N. J., *Lab Chip* **2008,** *8* (4), 582-586.
[23] Fadeeva, E.; Truong, V. K.; Stiesch, M.; Chichkov, B. N.; Crawford, R. J.; Wang, J.; Ivanova, E. P., *Langmuir* **2011,** *27* (6), 3012-3019.
[24] Sousa, C.; Rodrigues, D.; Oliveira, R.; Song, W.; Mano, J. F.; Azeredo, J., *AMB Express* **2011,** *1*, 34-34.
[25] Anselme, K.; Davidson, P.; Popa, A. M.; Giazzon, M.; Liley, M.; Ploux, L., *Acta Biomater.* **2011,** *7* (4), 1936-1937.
[26] Quan, Y.-Y.; Zhang, L.-Z.; Qi, R.-H.; Cai, R.-R., *Scientific Reports* **2016,** *6* (1), 38239.
[27] Imani, S. M.; Maclachlan, R.; Rachwalski, K.; Chan, Y.; Lee, B.; McInnes, M.; Grandfield, K.; Brown, E. D.; Didar, T. F.; Soleymani, L., *ACS Nano* **2020,** *14* (1), 454-465.
[28] Mateescu, M.; Knopf, S.; Mermet, F.; Lavalle, P.; Vonna, L., *Langmuir* **2020,** *36* (5), 1103-1112.
[29] Bakker, D. P.; Busscher, H. J.; van Zanten, J.; de Vries, J.; Klijnstra, J. W.; van der Mei, H. C., *Microbiology* **2004,** *150*, 1779-1784.
[30] Absolom, D.; Lamberti, F.; Policova, Z.; Zingg, W.; Oss, C.; Neumann, A., *Appl. Environ. Microbiol.* **1983,** *46*, 90-7.
[31] Boks, N. P.; Kaper, H. J.; Norde, W.; van der Mei, H. C.; Busscher, H. J., *J. Colloid Interface Sci.* **2009,** *331* (1), 60-64.
[32] He, B.; Lee, J.; Patankar, N. A., *Colloids and Surfaces A: Physicochemical and Engineering Aspects* **2004,** *248* (1), 101-104.
[33] Nosonovsky, M.; Bhushan, B., *Adv. Funct. Mater.* **2008,** *18* (6), 843-855.
[34] Zhang, X.; Wang, L.; Levanen, E., *RSC Advances* **2013,** *3* (30), 12003-12020.
[35] Crawford, R. J.; Webb, H. K.; Truong, V. K.; Hasan, J.; Ivanova, E. P., *Adv. Colloid Interface Sci.* **2012,** *179-182*, 142-149.

[36] Mertz, G.; Delmée, M.; Bardon, J.; Martin, A.; Ruch, D.; Fouquet, T.; Garreau, S.; Airoudj, A.; Marguier, A.; Ploux, L.; Roucoules, V., *Plasma Processes Polym.* **2018,** *15* (10), 1800073.
[37] Miao, H.; Ratnasingam, S.; Pu, C. S.; Desai, M. M.; Sze, C. C., *J. Microbiol. Methods* **2009,** *76* (2), 109-119.
[38] Farhi, R.; Morel, C.; Chéron, J., Institut National de Recherche et Sécurité (France): 2006.
[39] Parvate, S.; Dixit, P.; Chattopadhyay, S., *The Journal of Physical Chemistry B* **2020,** *124* (8), 1323-1360.
[40] Whitehead, K. A.; Verran, J., *Food and Bioproducts Processing* **2006,** *84* (4), 253-259.
[41] Truong, V. K.; Lapovok, R.; Estrin, Y. S.; Rundell, S.; Wang, J. Y.; Fluke, C. J.; Crawford, R. J.; Ivanova, E. P., *Biomaterials* **2010,** *31* (13), 3674-3683.
[42] Stout, K. J.; Blunt, L.; Dong, W. P.; Mainsah, E.; Luo, N.; Mathia, T.; Sullivan, P. J.; Zahouani, H., Elsevier Science: 2000.
[43] Wenzel, R. N., *Industrial & Engineering Chemistry* **1936,** *28* (8), 988-994.
[44] Quéré, D., *Physica A: Statistical Mechanics and its Applications* **2002,** *313* (1), 32-46.
[45] Søgaard, E.; Andersen, N. K.; Smistrup, K.; Larsen, S. T.; Sun, L.; Taboryski, R., *Langmuir* **2014,** *30* (43), 12960-12968.
[46] Wang, J.; Yang, Q.; Wang, M.; Wang, C.; Jiang, L., *Soft Matter* **2012,** *8* (7), 2261-2266.
[47] Bhushan, B.; Nosonovsky, M., *Philosophical Transactions of the Royal Society A: Mathematical, Physical and Engineering Sciences* **2010,** *368* (1929), 4713-4728.
[48] Hisler, V.; Vonna, L.; Le Houerou, V.; Knopf, S.; Gauthier, C.; Nardin, M.; Haidara, H., *Langmuir* **2014,** *30* (31), 9378-9383.
[49] Nosonovsky, M.; Bhushan, B., Springer-Verlag: Berlin Heidelberg, 2012.
[50] Barthlott, W.; Neinhuis, C., *Planta* **1997,** *202* (1), 1-8.
[51] Hisler, V.; Jendoubi, H.; Hairaye, C.; Vonna, L.; Le Houérou, V.; Mermet, F.; Nardin, M.; Haidara, H., *Langmuir* **2016,** *32* (31), 7765-7773.
[52] Kleingartner, J. A.; Srinivasan, S.; Mabry, J. M.; Cohen, R. E.; McKinley, G. H., *Langmuir* **2013,** *29* (44), 13396-13406.
[53] Vinogradova, O. I.; Dubov, A. L., *Mendeleev Commun.* **2012,** *22* (5), 229-236.
[54] Zhu, H.; Guo, Z.; Liu, W., *Chem. Commun.* **2014,** *50* (30), 3900-3913.
[55] Bhushan, B.; Jung, Y. C.; Koch, K., *Philos Trans A Math Phys Eng Sci* **2009,** *367* (1894), 1631-72.
[56] Kirk, S.; Strobel, M.; Lee, C.-Y.; Pachuta, S. J.; Prokosch, M.; Lechuga, H.; Jones, M. E.; Lyons, C. S.; Degner, S.; Yang, Y.; Kushner, M. J., *Plasma Processes Polym.* **2010,** *7* (2), 107-122.
[57] Zhao, Q., *Surf. Coat. Technol.* **2004,** *185* (2-3), 199-204.
[58] Ishihara, M.; Kosaka, T.; Nakamura, T.; Tsugawa, K.; Hasegawa, M.; Kokai, F.; Koga, Y., *Diamond Relat. Mater.* **2006,** *15* (4-8), 1011-1014.
[59] Ploux, L.; Beckendorff, S.; Nardin, M.; Neunlist, S., *Colloids and Surfaces B: Biointerfaces* **2007,** *57*, 174-181.
[60] Katsikogianni, M.; Spiliopoulou, I.; Dowling, D. P.; Missirlis, Y. F., *J. Mater. Sci.: Mater. Med.* **2006,** *17* (8), 679-689.
[61] Hsu, L. C.; Fang, J.; Borca-Tasciuc, D. A.; Worobo, R. W.; Moraru, C. I., *Appl. Environ. Microbiol.* **2013,** *79* (8), 2703.
[62] Anselme, K.; Davidson, P.; Popa, A. M.; Giazzon, M.; Liley, M.; Ploux, L., *Acta Biomater.* **2010,** *6* (10), 3824–3846.

[63] Svensson, S.; Forsberg, M.; Hulander, M.; Vazirisani, F.; Palmquist, A.; Lausmaa, J.; Thomsen, P.; Trobos, M., *Int. J. Nanomedicine* **2014,** *9*, 775-94.
[64] Azeredo, J.; Azevedo, N. F.; Briandet, R.; Cerca, N.; Coenye, T.; Costa, A. R.; Desvaux, M.; Di Bonaventura, G.; Hébraud, M.; Jaglic, Z.; Kačániová, M.; Knøchel, S.; Lourenço, A.; Mergulhão, F.; Meyer, R. L.; Nychas, G.; Simões, M.; Tresse, O.; Sternberg, C., *Crit. Rev. Microbiol.* **2017,** *43* (3), 313-351.
[65] Busscher, H. J.; Weerkamp, A. H.; van der Mei, H. C.; van Pelt, A. W.; de Jong, H. P.; Arends, J., *Appl. Environ. Microbiol.* **1984,** *48* (5), 980-983.
[66] Böhmler, J.; Haidara, H.; Ponche, A.; Ploux, L., *ACS Biomaterials Science & Engineering* **2015,** *1* (8), 693-704.
[67] Luo, C.; Zheng, H.; Wang, L.; Fang, H.; Hu, J.; Fan, C.; Cao, Y.; Wang, J., *Angewandte Chemie International Edition* **2010,** *49* (48), 9145-9148.
[68] Papadopoulos, P.; Deng, X.; Vollmer, D.; Butt, H.-J., *J. Phys.: Condens. Matter* **2012,** *24* (46), 464110.
[69] Chen, G.; Strevett, K. A., *Environ. Microbiol.* **2001,** *3* (4), 237-45.
[70] Hermansson, M., *Colloids and Surfaces B: Biointerfaces* **1999,** *14*, 105-119.
[71] Carniello, V.; Peterson, B. W.; van der Mei, H. C.; Busscher, H. J., *Adv. Colloid Interface Sci.* **2018,** *261*, 1-14.
[72] Lecuyer, S.; Rusconi, R.; Shen, Y.; Forsyth, A.; Vlamakis, H.; Kolter, R.; Stone, H. A., *Biophys. J.* **2011,** *100* (2), 341-50.
[73] Petersen, J.; Becker, C.; Fouquet, T.; Addiego, F.; Toniazzo, V.; Dinia, A.; Ruch, D., *RSC Advances* **2013,** *3* (13), 4416-4424.
[74] Beamson, G.; Briggs, D., *J. Chem. Educ.* **1993,** *70* (1), A25.
[75] Briggs, D., Cambridge University Press: Cambridge, 1998.
[76] Gualdi, L.; Tagliabue, L.; Bertagnoli, S.; Ieranò, T.; De Castro, C.; Landini, P., *Microbiology* **2008,** *154* (7), 2017-2024.
[77] Christensen, G. D.; Bisno, A. L.; Parisi, J. T.; McLaughlin, B.; Hester, M. G.; Luther, R. W., *Ann. Intern. Med.* **1982,** *96* (1), 1-10.
[78] Mauclaire, L.; Brombacher, E.; Bünger, J. D.; Zinn, M., *Colloids and Surfaces B: Biointerfaces* **2010,** *76* (1), 104-111.
[79] Vidal, O.; Longin, R.; Prigent-Combaret, C.; Dorel, C.; Hooreman, M.; Lejeune, P., *J. Bacteriol.* **1998,** *180* (9), 2442-2449.
[80] Rasband, W., U. S. National Institutes of Health, Bethesda, Maryland, USA, 1997.
[81] Prévost, V.; Anselme, K.; Gallet, O.; Hindié, M.; Petithory, T.; Valentin, J.; Veuillet, M.; Ploux, L., *ACS Biomaterials Science & Engineering* **2019**.
[82] Böhmler, J.; Haidara, H.; Ponche, A.; Ploux, L., *ACS Biomaterials Science & Engineering* **2015,** *2015* (1), 693–704.
[83] Dorobantu, L. S.; Gray, M. R., *Scanning* **2010,** *32* (2), 74-96.
[84] Krishnan, A.; Liu, Y.-H.; Cha, P.; Woodward, R.; Allara, D.; Vogler, E. A., *Colloids and Surfaces B: Biointerfaces* **2005,** *43* (2), 95-98.
[85] Young, T. J.; Monclus, M. A.; Burnett, T. L.; Broughton, W. R.; Ogin, S. L.; Smith, P. A., *Meas. Sci. Technol.* **2011,** *22* (12), 125703.
[86] Reyssat, M.; Pépin, A.; Marty, F.; Chen, Y.; Quéré, D., *Europhys. Lett.* **2006,** *74* (2), 306-312.
[87] Rioboo, R.; Voué, M.; Vaillant, A.; De Coninck, J., *Langmuir* **2008,** *24* (24), 14074-14077.

Table 1: Chemical composition of coating surfaces ranging from 0 to 100% actual %PFDA, as determined by XPS survey (C1s, F1s, O1S, Si2p) and C1s High-Resolution analyses. Coatings are displayed as %PFDA classes of 20%.

	%area on Survey Spectrum				%area on High-Resolution Spectrum					
%PFDA	**C1s**	**F1s**	**O1s**	**Si2p**	**CHx C-C** 285.28 eV	**C-O** 286.96 eV	**O=C-O** 289.07 eV	**(-CF2-)** 291.35 eV	**CF2-CF3** 293.71 eV	**CFx-CF-CFx** 288.74 eV
0	88 ± 2	-	9 ± 3	-	87	6	6	-	-	-
20-39	75 ± 2	14 ± 1	11 ± 2	-	79 ± 3	8 ± 1	6 ± 1	5 ± 1	1	-
40-59	59 ± 3	32 ± 3	8	-	69 ± 3	8	7	14 ± 3	2	0.3 ± 0.1
60-79	51 ± 2	42 ± 2	7	-	54 ± 3	8	6	27 ± 2	4	0.8 ± 0.1
80-99	42 ± 2	51 ± 3	7	-	32 ± 5	8 ± 1	7 ± 1	43 ± 5	6 ± 1	1
100	39 ± 1	55 ± 1	6 ± 1	-	22 ± 1	8 ± 1	7 ± 1	52 ± 2	8 ± 1	2 ± 1
PP	91 ± 1	-	6 ± 20	2	-	-	-	-	-	-
SW	9	-	25 ± 1	65 ± 1	-	-	-	-	-	-

Table 2: Summary of the main parameters used to describe chemistry, topography, wettability and mechanical properties of the coatings and reference surfaces.

Material property	Parameter	Meaning	Bibliographic reference
Chemistry	C1s, F1s, O1s, Si1s	% of atom in coating	[75]
	$\underline{C}H_x$ and $\underline{C}$-C / Ctot	DOCA content	[36] [75]
	$\underline{C}$-O / Ctot	Polymerization	
	O=$\underline{C}$-O / Ctot	Polymerization	
	(-$\underline{C}F_2$-) / Ctot	PFDA content	
	CF_2-$\underline{C}F_3$ / Ctot	PFDA content	
	CF_x-$\underline{C}F$-CF_x / Ctot	Coupling of PFDA content & Polymerization	
Topography	Sa	Roughness Average (amplitude)	[42] [83] [40]
	Sq	Root Mean Square (amplitude)	
	Sz	Peak-Peak Height (amplitude)	
	Ssk	Surface Skewness (symmetry) [a]	
	Spk/Svk	Reduced Height Ratio of Summit with Valley (symmetry) [b]	
	Sk, Sv, Sp	Other Amplitude parameters	
	Sku	Surface Kurtosis (amplitude) [c]	
	Sds	Density of Summits (spatial)	
	Ssc	Mean Summit Curvature (hybrid) [d]	
	Sdr	Surfaces developed Ratio (hybrid) [e]	
	Sfd, Sdq,Sbi ,Sci ,Svi	Functional Parameters	
Wettability	θ*	Static water angle	[84]
	θ^A	Advancing water angle	
	θ^R	Receding water angle	
	Δθ	Hysteresis (θ^A-θ^R)	
Mechanical	Young modulus	Stiffness	[85]

a) Asymmetry of the height distribution histogram: (i) if Ssk = 0, symmetric height distribution, (ii) if Ssk < 0, bearing surface with holes and (ii) if Ssk > 0, flat surface with peaks.
b) Quantity of peak structures relative to valley structures for surfaces with similar Sa surface roughness.
c) Sharpness of the surface topography: if Sku < 3, broad and blunt peaks, if Sku > 3, narrow and sharp peaks.
d) Hybrid shall be understood as a combination of amplitude and spatial information.
e) Ratio between the actual interfacial surface area relative to area of the projected (flat) x,y plane. For a flat surface, surface area and area of x,y plane are equal and Sdr = 0%.

Table 1 : Topographic description of PFDA/DOCA coating surfaces ranging from 0 to 100% actual %PFDA based on the principal topography parameters measured on AFM images of 10 µm x 10 µm (average over 3 locations on 3 samples).

	Morphology					**Texture**			
%PFDA	**Sa (nm)**	**Sq (nm)**	**Sz (nm)**	**Ssk (-)**	**Spk/Svk (-)**	**Sku (-)**	**Sds ($1/\mu m^2$)**	**Ssc (10^{-3}/nm)**	**Sdr (%)**
0	44 ± 29	56 ± 34	428 ± 55	-	-	-	-	-	-
20-39	130 ± 18	198 ± 22	1054 ± 99	0.6 ± 0.5	2.0 ± 0.8	3 ± 1	2 ± 1	7.0 ± 0.3	6 ± 3
40-59	146 ± 14	190 ± 13	1229 ± 89	0.8 ± 0.1	3.0 ± 0.9	4.0 ± 0.1	3 ± 1	11	13 ± 10
60-79	124 ± 37	159 ± 9	866 ± 47	0.5 ± 0.2	3 ± 1	3 ± 1	4.0 ± 0.5	4.0 ± 0.3	25 ± 6
80-99	144 ± 11	181 ± 13	1380 ± 95	0.7 ± 0.1	2.0 ± 0.5	8 ± 2	6 ± 2	5 ± 2	130 ± 25
100	139 ± 8	180 ± 19	1485 ± 88	0.8 ± 0.1	3 ± 1	4.0 ± 0.2	9 ± 1	9.0 ± 0.3	150 ± 30
PP	16 ± 1	20 ± 1	116 ± 20	-	-	-	-	-	-
SW	11	14	126 ± 10	-	-	-	-	-	-

Table 4: Output data of *model*^{0} and *model*^{2}. Models are with or without interactions according to AIC values. Retained variables are variables retained after VIFs-based selection, classified in the decreasing impact ranking according to the absolute value of their load impact. *, ** and ***: significance based on the *p*-value.

Model & Conditions	Retained variables	Load impact (LI)	Standard deviation on LI	*p*-value
***model*^{0}**	Media	-30.6	0.3	< 0.001 ***
	Time	16.0	0.5	< 0.001 ***
	Strain	-6.6	0.8	< 0.001 ***
	CFx	-3.0	0.6	< 0.001 ***
	O1s, C-O, O=C-O, Δθ, θ^{A}, Sq, Ssk, Sdr	< 1.0	-	> 0.05
***model*^{2}** *E. coli* NaCl 1h	Ssk	-110	38	0.001 **
	Sdr : Ssk	-109	45	0.016 *
	Δθ : Ssk	33	15	0.034 *
	Sdr	-32	11	0.001 **
	Sq : Sdr	9	3	0.002 **
	Δθ	8	3	0.012 *
	Sq	7	3	0.014 *
	O=C-O	6	2	0.010 *
	O1s	4	1	0.004 **
	C-O	2	1	0.025 *
***model*^{2}** *E. coli* NaCl 3h	Sdr : Ssk	-88	26	0.001 **
	Ssk	-42	12	< 0.001 ***
	Sdr	-21	6	< 0.001 ***
	Sq	5	1	< 0.001 ***
	Sq : Sdr	5	1	0.001 **
***model*^{2}** *E. coli* NaCl 24h	Sq	< 1	-	> 0.05
***model*^{2}** *E. coli* M63G 1h	Δθ	1.8	0.4	< 0.001 ***
	CFx	-1.1	0.4	0.042 *
***model*^{2}** *E. coli* LB 1h	Δθ	1.2	0.4	0.007 **

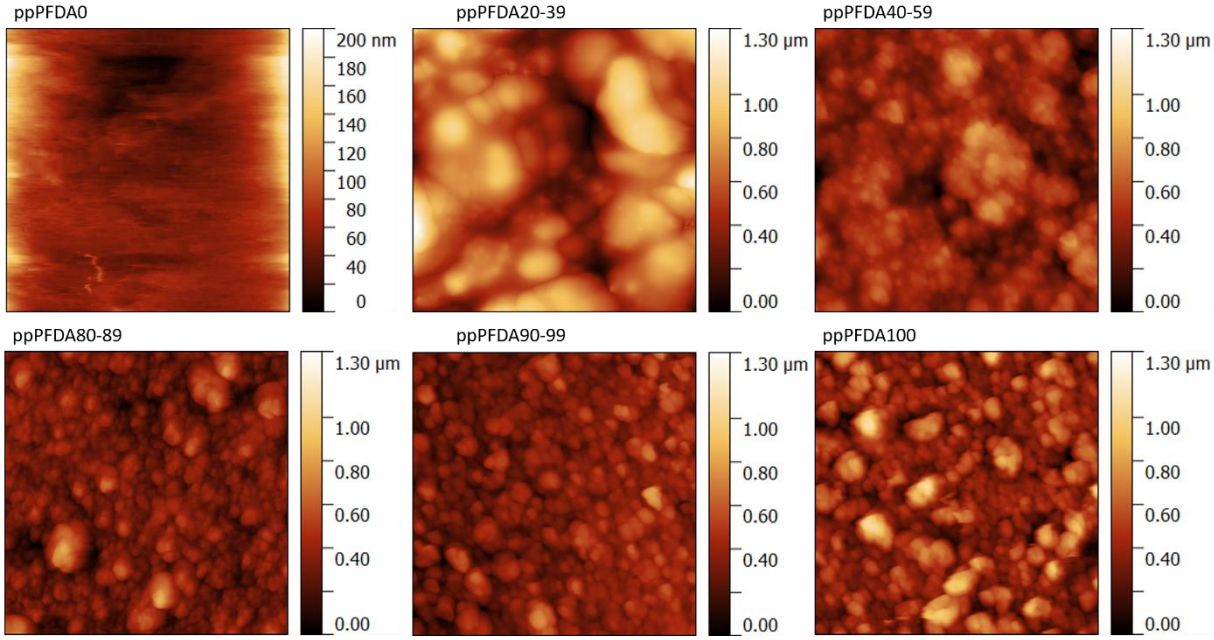

Figure 1: 10 µm × 10 µm topographical AFM images of PFDA/DOCA coatings typical for the different %PFDA at the extreme surface.

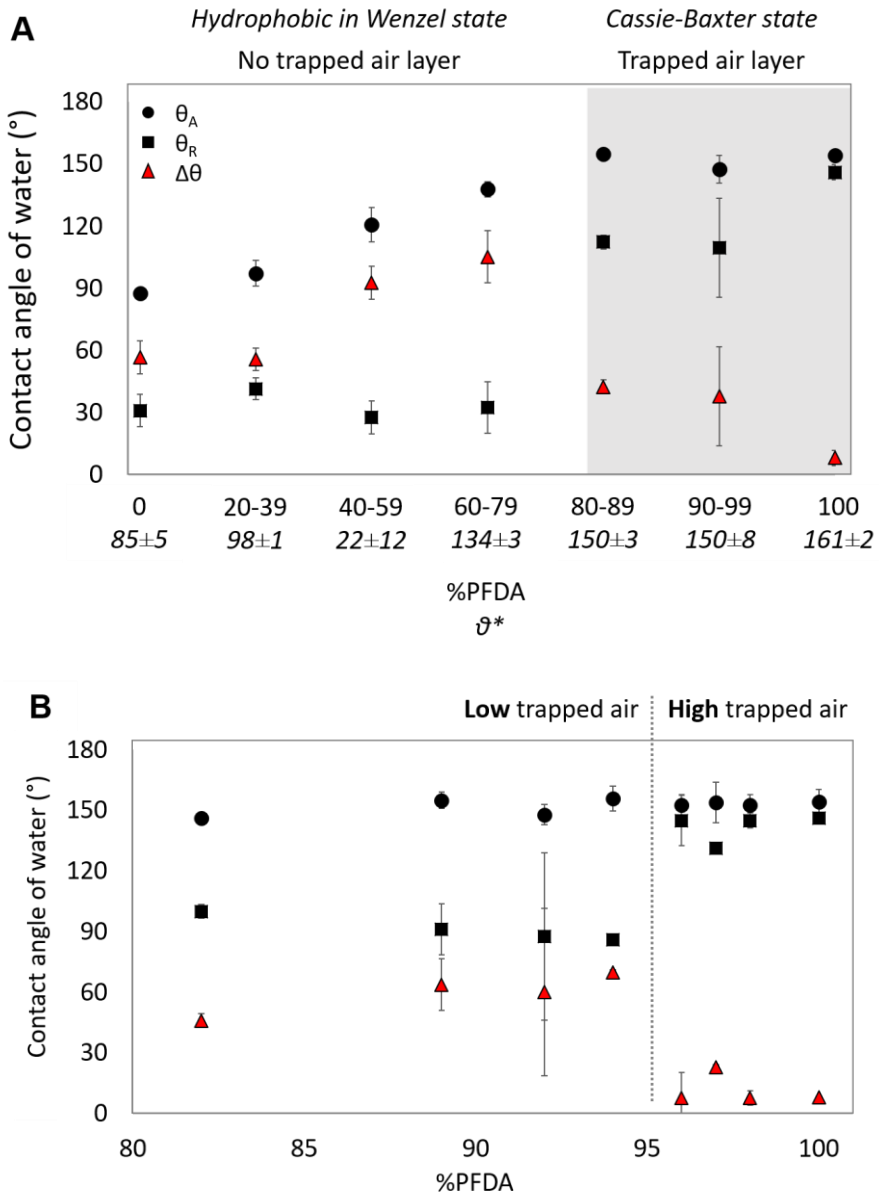

Figure 2: Contact angle of water, static θ*, advancing θ_A, receding θ_R angles and hysteresis Δθ measured on coatings with %PFDA **(A)** from 0 to 100%, and **(B)** more precisely from 80 to 100%.

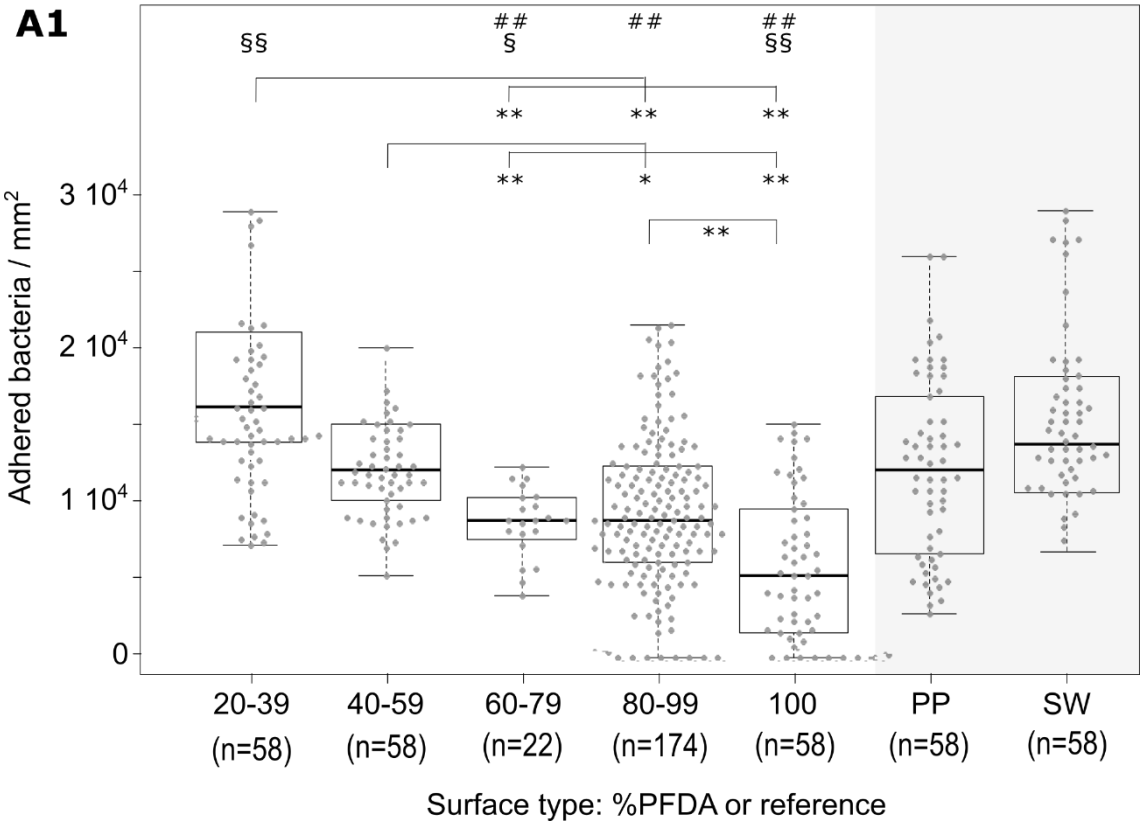
A1
Adhered bacteria / mm2
3 10^4
2 10^4
1 10^4
0
20-39 (n=58)
40-59 (n=58)
60-79 (n=22)
80-99 (n=174)
100 (n=58)
PP (n=58)
SW (n=58)
Surface type: %PFDA or reference

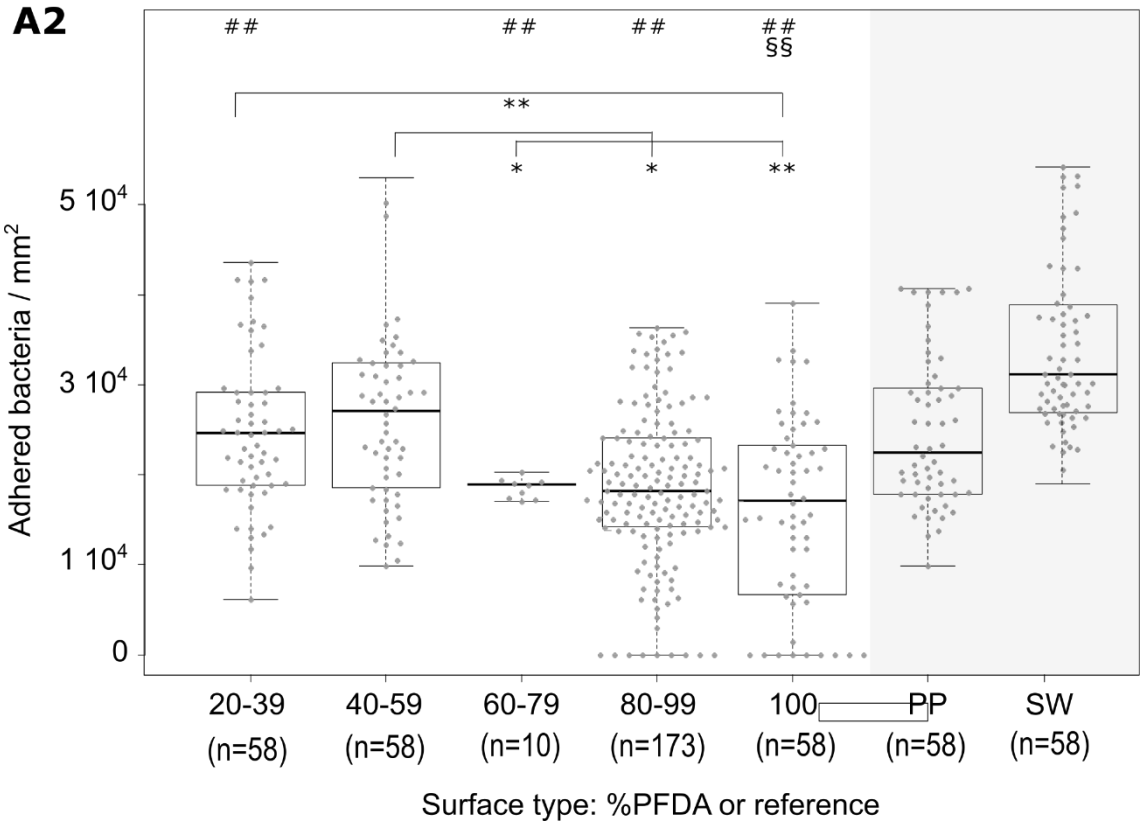
A2
Adhered bacteria / mm2
5 10^4
3 10^4
1 10^4
0
20-39 (n=58)
40-59 (n=58)
60-79 (n=10)
80-99 (n=173)
100 (n=58)
PP (n=58)
SW (n=58)
Surface type: %PFDA or reference

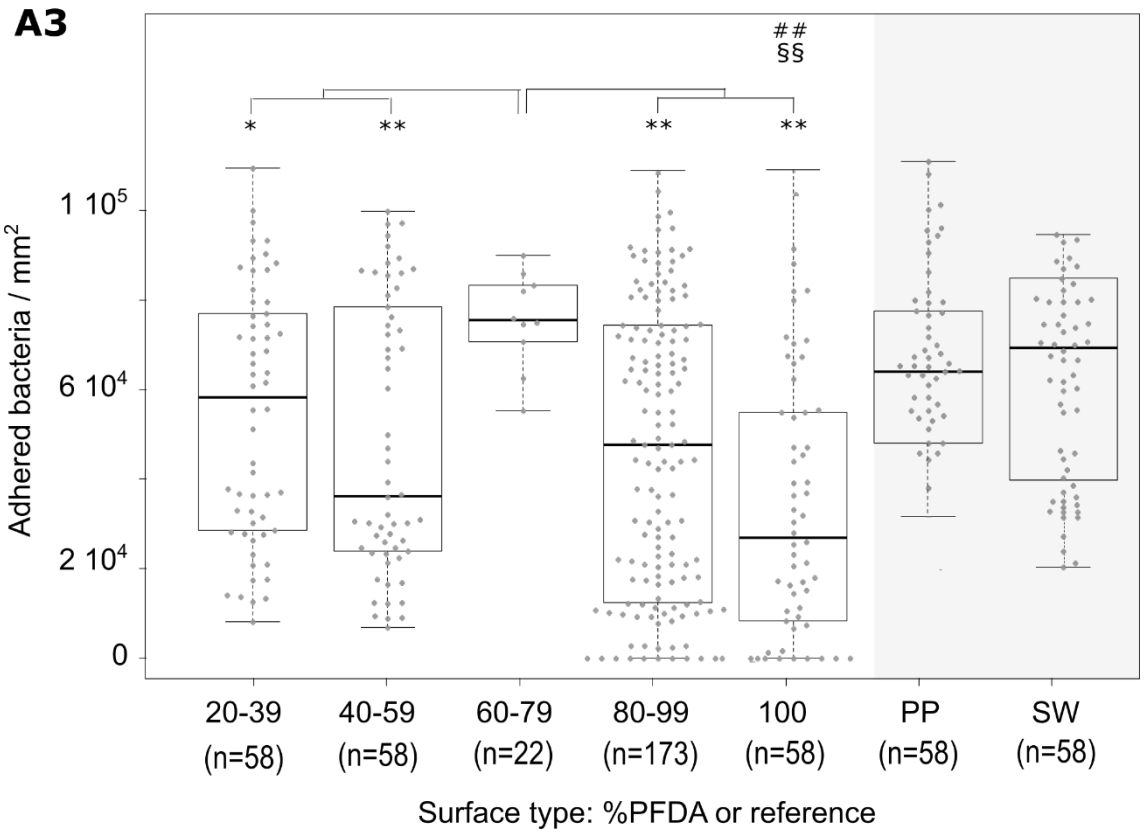
A3
##
§§
*
**
**
**
1 10^5
6 10^4
2 10^4
0
Adhered bacteria / mm^2
20-39 (n=58)
40-59 (n=58)
60-79 (n=22)
80-99 (n=173)
100 (n=58)
PP (n=58)
SW (n=58)
Surface type: %PFDA or reference

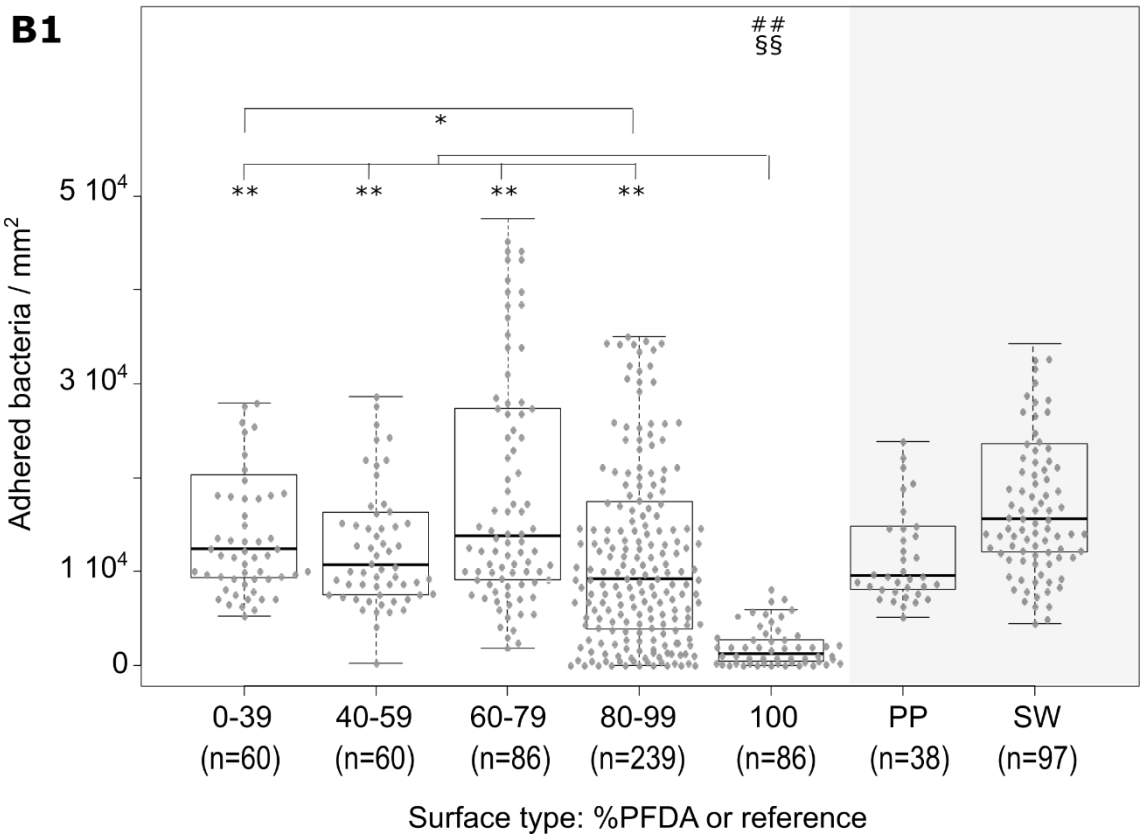
B1
##
§§
*
**
**
**
**
5 10^4
3 10^4
1 10^4
0
Adhered bacteria / mm^2
0-39 (n=60)
40-59 (n=60)
60-79 (n=86)
80-99 (n=239)
100 (n=86)
PP (n=38)
SW (n=97)
Surface type: %PFDA or reference

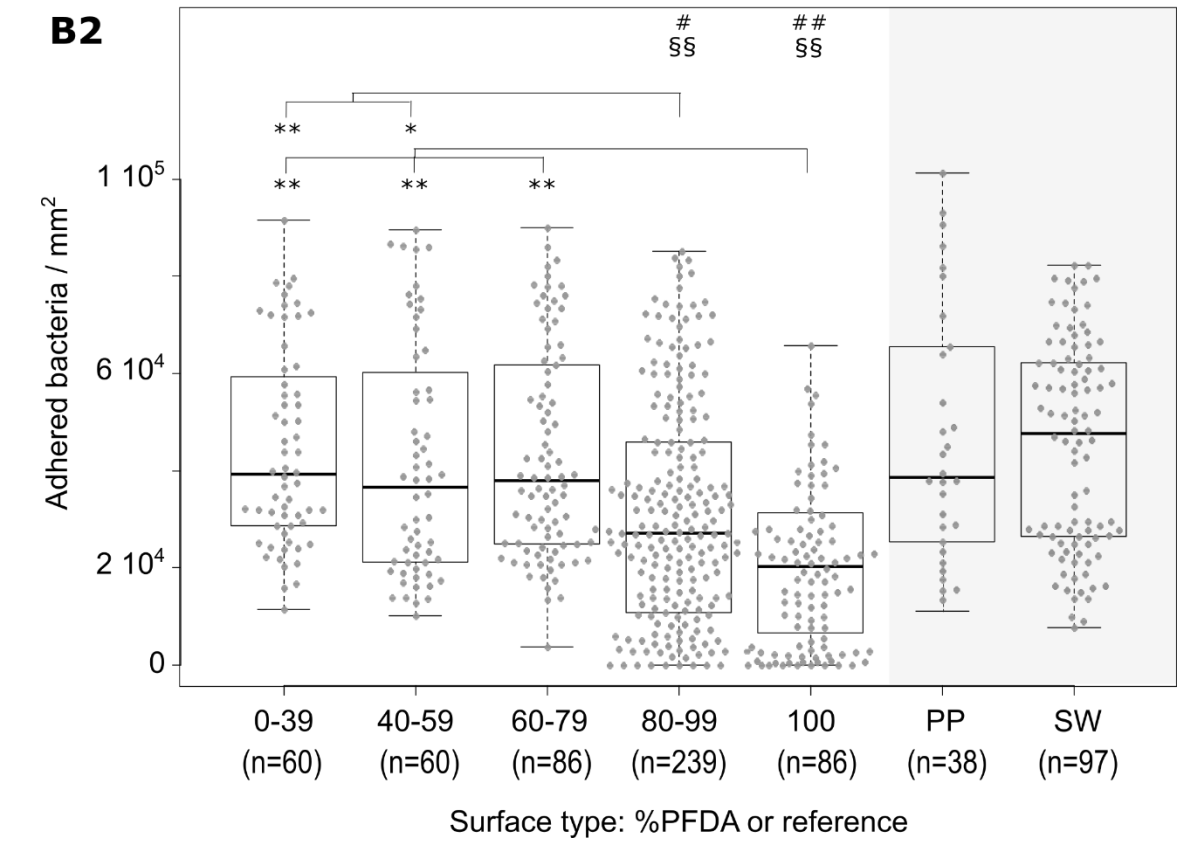

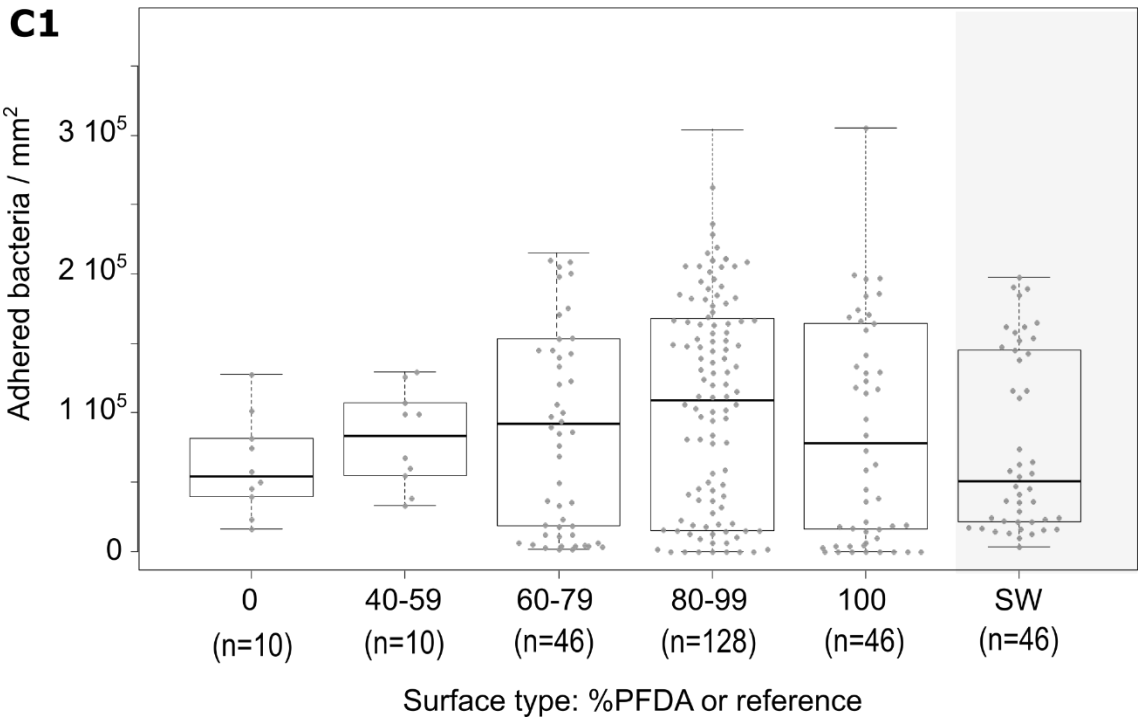

Figure 3: Number of *E. coli* bacteria adhered on coatings of different %PFDA and on SW and PP reference surfaces: **(A1, A2, A3)** after 1h, 3h and 24h of culture in NaCl medium, **(B1, B2)** after 1h and 3h of *E. coli* culture in M63G medium, **(C1)** after 1h of culture in LB medium. ##

and #: Significant difference compared to SW ($\alpha < 0.01$ and $\alpha < 0.05$); §§ and §: Significant difference compared to PP ($\alpha < 0.01$ and $\alpha < 0.05$); ** and *: Significant difference between coatings ($\alpha < 0.01$ and $\alpha < 0.05$). n: number of values for a given surface in the given conditions.

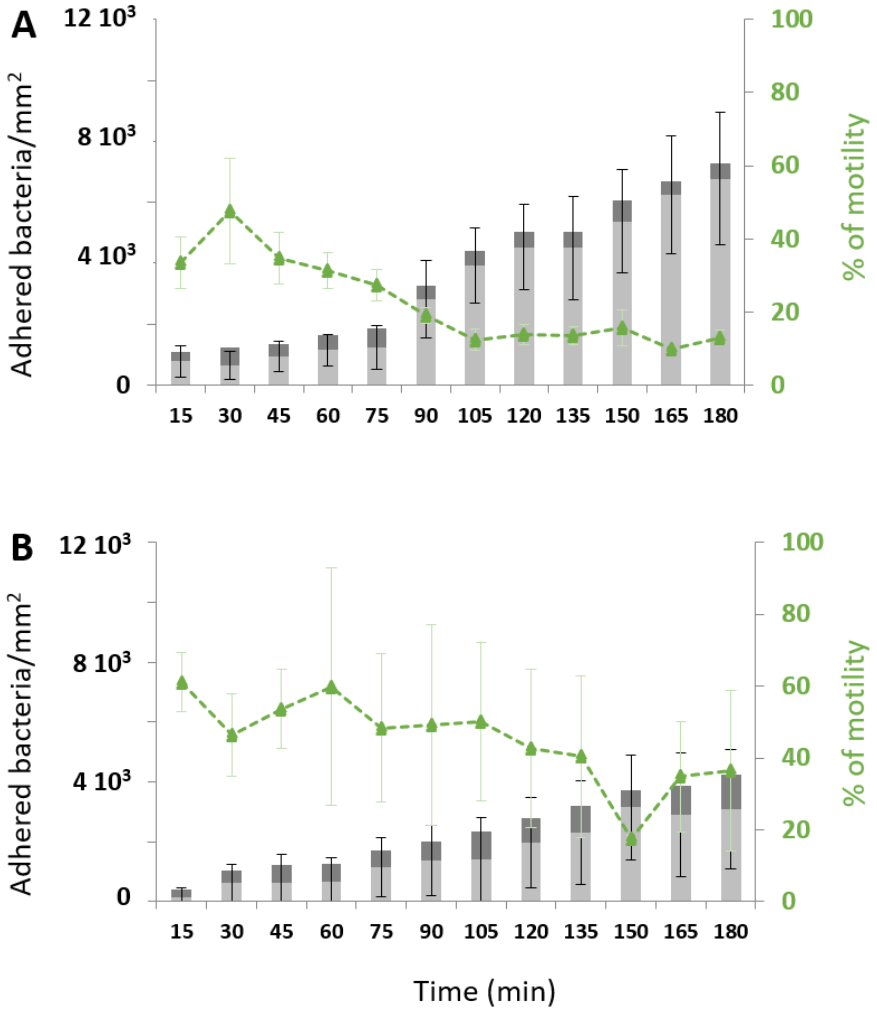

Figure 4: Mobility and growth of *E. coli* bacteria on ppPFDA20-39 **(A)** and ppPFDA100 **(B)** coatings over 3h of culture in NaCl 9g/L medium in a home-made real-time imaging setup for an up-right fluorescence confocal microscope **(Figure S5A)**. Number of mobile and non-mobile bacteria are displayed in the dark and light grey bin categories respectively. Fraction of

the mobile bacterial population among the total population measured in contact with the coating surface is displayed by the curve with green ▲ symbol.

Table of contents

A crucial topic of biomedical applications of low-wettable and superhydrophobic coatings is adressed with regard to their interface with bacteria when immersed in liquid. Aside from describing the conditions favorable to reduction in colonization, causal factors are determined by GLMM-based statistical analysis. The biointerface is controlled by culture conditions and secondary by surface topography. Air trapping plays a role on a local scale, preserving bacteria-free areas even in clogging conditions.

Keyword : Biointerface with bacteria

Authors: Adeline Marguier, Nicolas Poulin, Charline Soraru, Laurent Vonna, Samar Hajjar-Garreau, Philippe Kunemann, Aissam Airoudj, Grégory Mertz, Julien Bardon, Maxime Delmée, Vincent Roucoules, David Ruch, Lydie Ploux*

Title: Bacterial colonization of low-wettable surfaces is driven by culture conditions and topography

ToC figure: (110 mm broad × 20 mm high)

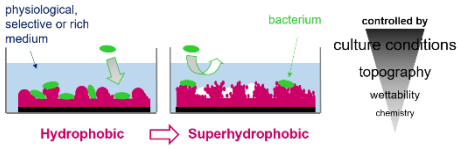

Supporting Information

Bacterial colonization of low-wettable surfaces is driven by culture conditions and topography

*Adeline Marguier, Nicolas Poulin, Charline Soraru, Laurent Vonna, Samar Hajjar-Garreau, Philippe Kunemann, Aissam Airoudj, Grégory Mertz, Julien Bardon, Maxime Delmée, Vincent Roucoules, David Ruch, Lydie Ploux**

Table S1: Hysteresis (Δθ) measured on ppPFDA100 coatings before (T0) and 3h (T0 + 3h), 24h (T0 + 24h) and 30 days (T0 + 30d) of immersion in NaCl or LB.

Medium	T0	T0 + 3h	T0 + 24h	T0 + 30d
NaCl	11 ± 5°	12 ± 2°	24 ± 4°	103 ± 3°
LB		98 ± 2°	102 ± 5°	-

Table S2: Explanatory variables **(A)** initially considered before VIFs-based selection, **(B)** retained after VIFs-based selection, and **(C)** results of the AIC analysis (AIC values i.e. quality of the statistical model) with or without taking into account interactions between the explanatory variables. This data is given for each of the models calculated in the study. In column (A), the *material-related variables* expression relates the following list of explanatory variables: %PFDA, C1s, F1s, O1s, CHx/C-C, C-O, O=C-O, CF2, CF2-CF3, CFx, θ*, θ^A, θ^R, Δθ, Sa, Sq, Ssk, Sku, Sz, Sds, Ssc, Sdq, Sdr, Sbi, Sci, Svi, Spk, Sk, Svk and Sfd. In column (C), values in bold highlight the lowest AIC values thus indicating the model version (with or without interactions) that must be retained.

Model & Conditions	**(A) Initial variables**	**(B) Variables retained after VIFs-based selection**	**(C) AIC values**	
			with interactions	**without interactions**
***model*^{0}**	*material-related variables* & Time, Species, Media	O1s, C-O, O=C-O, CFx, Δθ, θ^A, Sq, Ssk, Sdr, Time, Species, Media	14253	**14181**
***model*^{1}** *E. coli* NaCl	*material-related variables* & Time	C-O, Time	6681	**6677.8**
***model*^{1}** *E. coli* M63G	*material-related variables* & Time	CFx, Δθ, Sq, Time	5444	**4969**
***model*^{1}** *E. coli* & *S. epidermidis* LB	*material-related variables* & Species	CFx, Δθ, Species	1632	**1629**
***model*^{2}** *E. coli*	*material-related variables*	O=C-O, Δθ, Sq, Sdr	**1817.7**	1911.5

NaCl 1h				
model² *E. coli* NaCl 3h	*material-related variables*	Δθ, Sdr	**2030.2**	2035.7
model² *E. coli* NaCl 24h	*material-related variables*	Δθ	2439.6	**2436.8**
model² *E. coli* M63G 1h	*material-related variables*	CFx, Δθ	2197.8	**2196.8**
model² *E. coli* M63G 3h	*material-related variables*	C-O, O=C-O, CFX, Sdr, Ssk	**2541.2**	2557.4
model² *E. coli* LB 1h	*material-related variables*	Δθ	-	**755.47**
model² *S. epidermidis* LB 1h	*material-related variables*	Sdr, %PFDA	**992**	-

Table S3: Output data of *model*[1] without interactions for *E. coli* in NaCl, for *E. coli* in M63G and for *E. coli* and *S. epidermidis* in LB. Models are without interactions according to AIC values (see Table 2). *Retained variables* in column (A) are variables retained after VIFs-based selection (see Table 2), classified in the impact ranking according to absolute value of their load impact. *, ** and ***: significance based on the *p*-value.

Model & Conditions	**Retained variables**	**Load impact (LI)**	**Standard deviation on LI**	***p*-value**
***model*[1]** *E. coli* NaCl	Time	12.469	0.426	< 0.01 ***
	C-O	0.265	0.418	< 0.01 ***
***model*[1]** *E. coli* M63G	Time	7.138	0.382	< 0.01 ***
	Δθ	1.440	0.402	< 0.01 ***
	CFx	-1.232	0.400	< 0.01 ***
	Sq	0.897	0.348	0.010 **
***model*[1]** *E. coli* & *S. epidermidis* LB	Species	-8.218	0.348	< 0.01 ***
	CFx	-6.462	0.400	< 0.01 ***
	Δθ	-0.063	0.402	0.014 **

Figure S1: Graphic definition of roughness parameters of particular relevance for this study: **(A)** Ssk is characteristic of the symmetry of the roughness shape, **(B)** Sku measures the sharpness of the roughness profile, **(C)** Spk/Svk determines quantitatively the dominance of peak structures relative to valley structures and **(D)** Sdr expresses the percentage of additional surface area contributed by the texture as compared to the projected area.

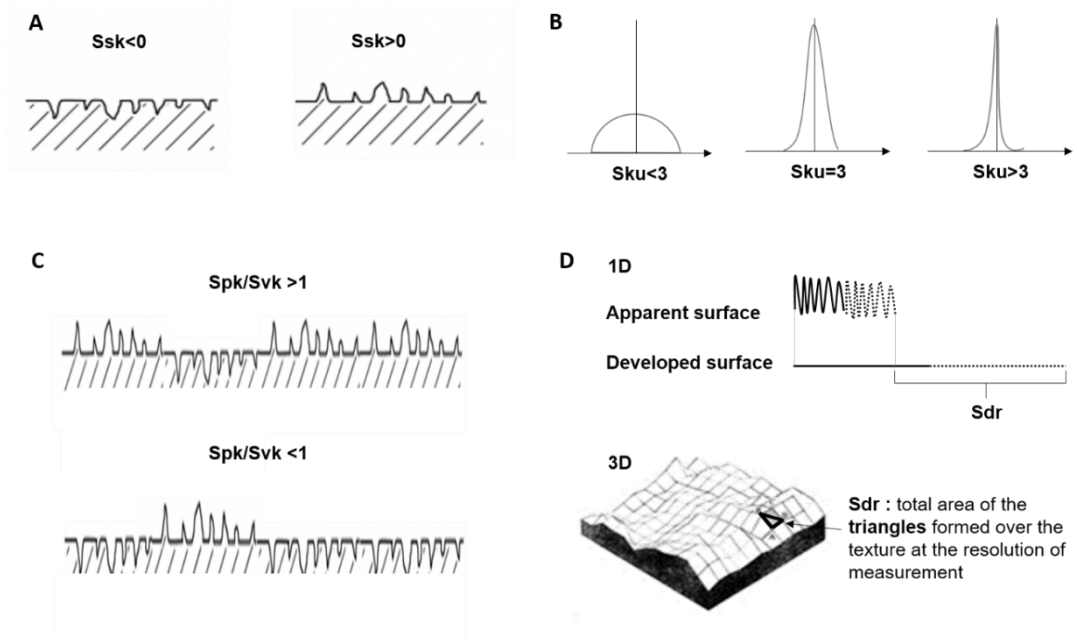

Figure S2: Topographical characteristics of the ppPFDAx coatings, with x from 0 to 100, determined on AFM images of 10 µm x 10 µm.

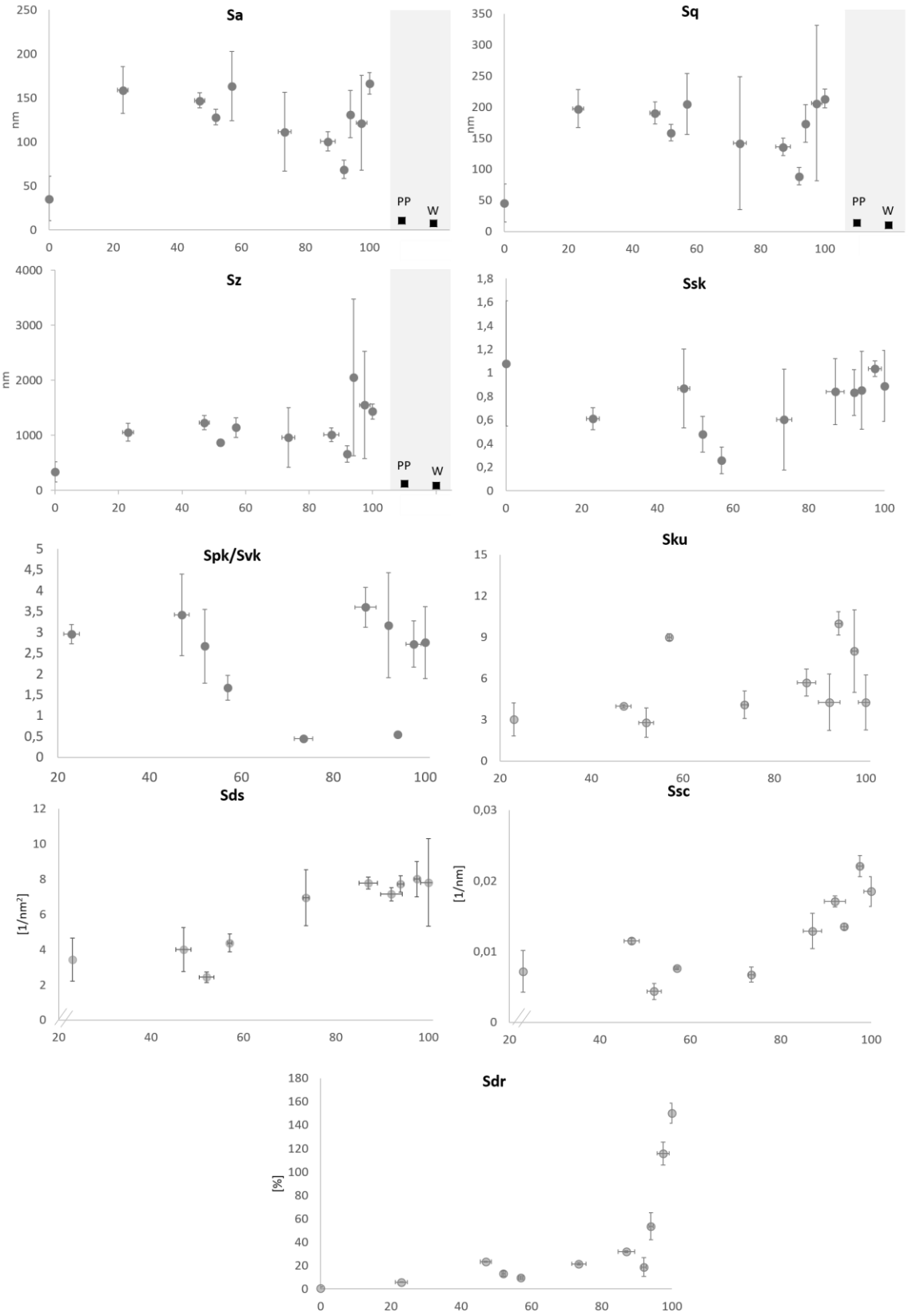

Figure S3: Bouncing of liquid drops onto the coatings was used to describe the forced wetting of the surface structuration. 5 µl drops were provided by a syringe through a capillary fiber allowing the production of constant drop diameter and volume. The impact was observed with a fast imaging system composed of 3 lamps (Flexilux universal®) illuminating the field of view and a NAF2× Teleplus MC4® camera fixed at 500 images s^{-1}. The set-up was designed for providing varying Weber number yet low enough to assure that bounce characterizes the interaction between liquid and substrate). The Weber number was determined with **equations S1** and **S2**, with ρ the liquid density, R the drop radius, γ the surface tension of the liquid, V the impact velocity, h the water column and g the standard gravity. The series of images were treated and analyzed by ImageJ® and Hiris® (CameraTool) software in order to extract contact time, spreading diameter, drop distortion and number of bounces. Bouncing on the coatings has been investigated with water, the three different culture media used in the study (NaCl, LB, M63G). Results are displayed as means of 3 independent measurements per sample. **(A)** Examples of photographs series showing bouncing of a water drop on ppPFDA, ppPFDA80 and ppDOCA surfaces for an impact velocity of 0.33 m s^{-1} (drop height of 2 cm); **(B)** Examples of the water column on ppPFDA89 and ppPFDA coatings, as well as wetting impact diameter and water column height for a 5 µl drop with velocity of 0.24 m s^{-1} (drop height of 6 cm, Weber number of 1.57) on coating with PFDA/DOCA content from 0 to 100% (mean of 3 measurements per sample; 2 samples per PFDA/DOCA content); **(C)** Variation of the water column height in relation to the Weber number, showing a maximal water column height varying with PFDA/DOCA content, which is characteristic of the capacity of the coating to retain water.[86-87]

$$W_e = \rho V^2 R/\gamma \quad \textbf{(S1)}$$

$$V = \sqrt{2gh}, \quad \textbf{(S2)}$$

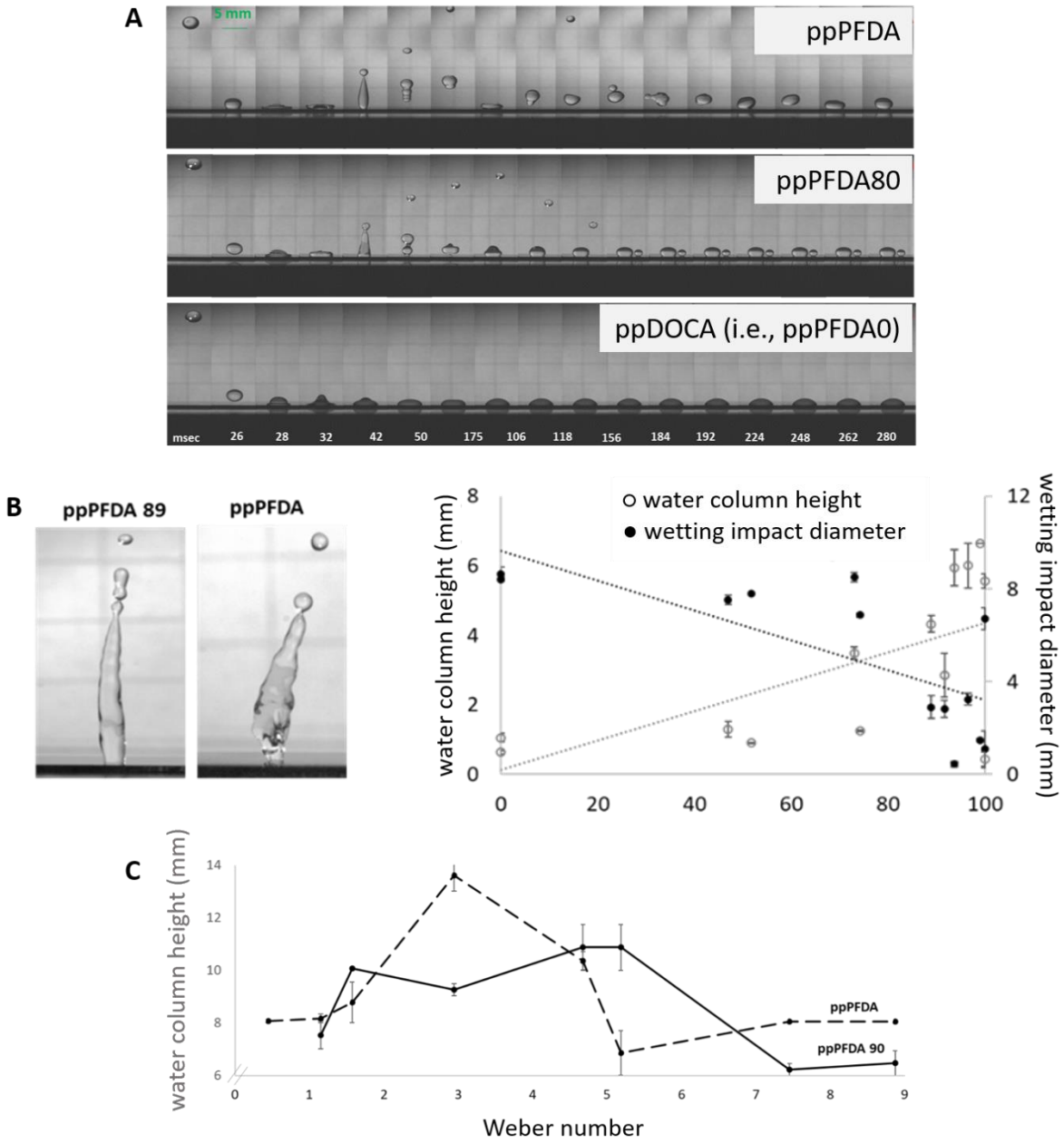
A
5 mm
ppPFDA
ppPFDA80
ppDOCA (i.e., ppPFDA0)
msec 26 28 32 42 50 175 106 118 156 184 192 224 248 262 280
B
ppPFDA 89
ppPFDA
water column height
wetting impact diameter
water column height (mm)
wetting impact diameter (mm)
0 2 4 6 8
0 4 8 12
0 20 40 60 80 100
C
water column height (mm)
6 8 10 12 14
0 1 2 3 4 5 6 7 8 9
Weber number
ppPFDA
ppPFDA 90

Figure S4: A Wilhelmy plate device (KRUSS modèle K12) equipped with a LabKrussDesktop® software was used to characterized the coating's wetting in conditions of complete immersion. The variation of the force needed to allow the material sample to penetrate the liquid (immersion) or to be removed from the liquid (emersion) is measured for a material composed of 2 identical coatings stuck together in a back-to-back position (LoctiteSuperglue3® cyanoacrylate glue). Measurements are done for a wetting perimeter of 20 mm × 10 mm. The capillary force being constant through immersion (or emersion) while the buoyant force varies according to the Archimede's principle, the total force provides the capillary force when the buoyant force equals zero. Total force-to-buoyant force results are thus extrapolated to extract the capillary forces for both immersion and emersion. Advancing (θ_A) and receding (θ_R) water contact angle measurements are finally calculated by **equation S3**, where F is the capillary force, L the wetting perimeter and γ_{LV} the surface tension of the liquid. Immersion/emersion cycles were repeated 3 times for each coating and each culture medium (M63G, NaCl et LB). **(A)** Capillary forces measures with ppPFDA80, ppPFDA90 and ppPFDA coatings in water and in a culture medium (LB). **(B)** Contact angle measurements calculated on this basis for ppPFDA80, ppPFDA90 and ppPFDA coatings in water and in LB medium.

$$F = L\gamma_{LV} \cos \theta \qquad \textbf{(S3)}$$

A

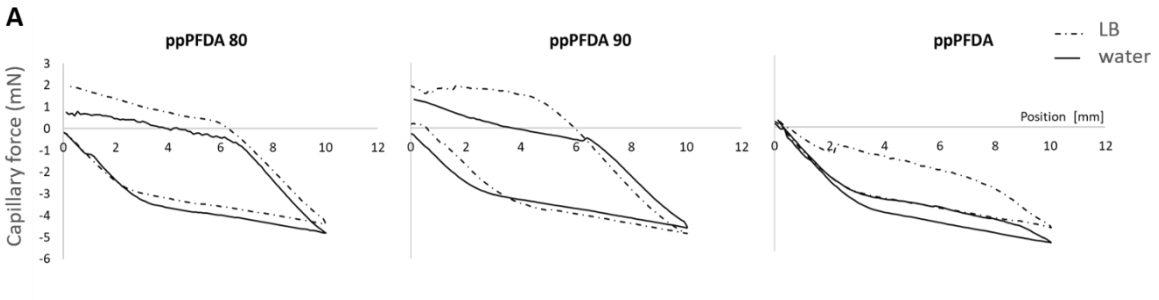

B

	ppPFDA80		ppPFDA90		ppPFDA	
	water	LB	water	LB	water	LB
θ_A (°)	156 ± 3	171 ± 10	153 ±8	175 ± 10	162 ± 15	163 ± 9
θ_R (°)	76 ± 8	30 ± 15	52 ± 20	59 ± 15	145 ± 10	83 ± 15
Δθ (°)	80 ± 10	136 ± 16	101 ± 18	116 ± 8	17 ± 8	80 ± 10

Figure S5: Surface tension of NaCl, M63G, LB and water has been evaluated with and without addition of bacterial cells, and wettability of the coating's surface has been characterized with the four liquids: **(A)** Surface tension of the four liquids without or with bacteria at a concentration of 5 10^6 CFU/mL as measured by the Wilhelmy plate method with a platine plate (mean of 3 independent measurements); **(B)** Changes with culture time in the surface tension of LB medium supplemented with 5 10^6 CFU/mL; **(C)** Contact angle measurements (θ* static, θ_A advancing, θ_R receding, Δθ hysteresis) on ppDOCA and ppPFDA coatings with the four liquids (water, NaCl, M63G, LB).

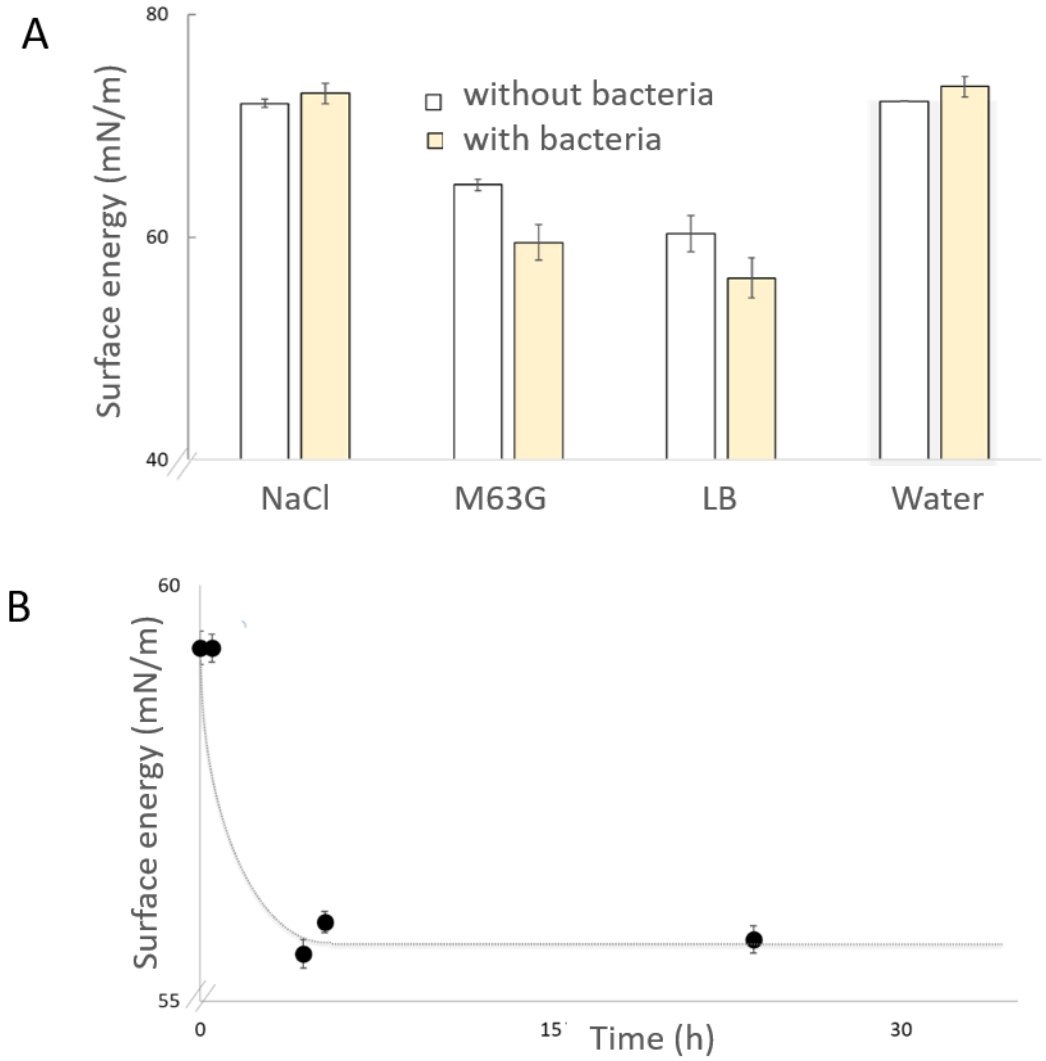

C	ppDOCA				ppPFDA			
	water	NaCl	M63G	LB	Water	NaCl	M63G	LB
θ^*	84 ± 4	84 ± 5	64 ± 7	65 ± 4	162 ± 2	164 ± 3	163 ± 4	163 ± 2
θ_A	97 ± 2	95 ± 2	75 ± 4	75 ± 4	154 ± 2	155 ± 3	155	159
θ_R	31 ± 8	18 ± 5	15 ± 5	21 ± 3	147 ± 5	151 ± 2	153 ± 1	154 ± 2
$\Delta\theta$	57 ± 9	52 ± 3	59 ± 3	77 ± 2	10 ± 3	11 ± 2	10 ± 1	7 ± 2

Figure S6: *Escherichia coli* SCC1 mobility and population growth on ppPFDA80-99 coatings **(B)** over 3h of culture in NaCl 9g/L medium. Measurements were performed with a home-made real-time imaging setup dedicated to an up-right fluorescence confocal microscope (Zeiss LSM700) **(A)**. Experimental setup is made of a culture chamber in which the three different coatings were placed. The culture chamber was installed under a x63 objective and was perfused with fresh medium over the culture duration according to a procedure described elsewhere (Böhmler, J.; Haidara, H.; Ponche, A.; Ploux, L., Impact of chemical heterogeneities of surfaces on colonization by bacteria. *ACS Biomaterials Science & Engineering* **2015,** *2015* (1), 693–704). Bacteria were injected just after acquisition was started and micrographs were taken every minute. Bacteria numbers were determined on micrographs as described in the Experimental Section. They are presented as their average for periods of 15 min (bin categories composed by the sum of in light and dark grey). Mobility of bacterial cells in contact with the surfaces was determined by using ImageJ® and plugins. Number of bacteria with displacement longer than the bacterial length (defined as mobile) is displayed in the dark bin categories. Number of non-mobile bacteria is displayed in light grey bin categories. Fraction of the mobile bacterial population among the total population measured in contact with the coating surface is displayed by the curve with green ▲ symbol.

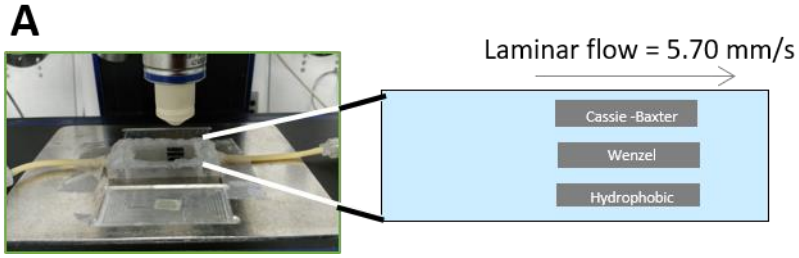

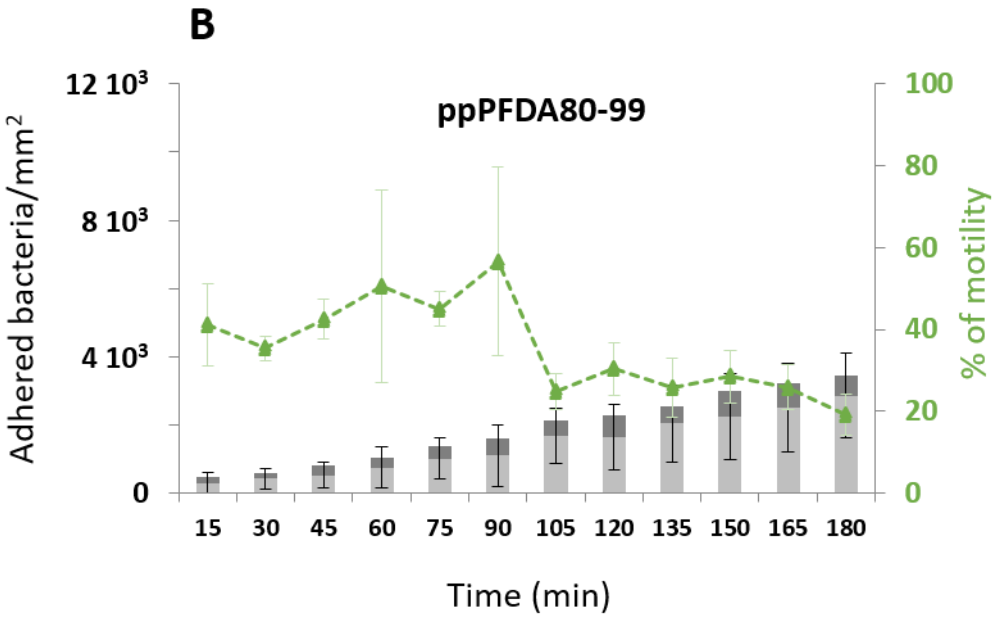
B
ppPFDA80-99
Adhered bacteria/mm²
12 10³
8 10³
4 10³
0
100
80
60
40
20
0
% of motility
15
30
45
60
75
90
105
120
135
150
165
180
Time (min)

Figure S7: (A) Photograph of a ppPFDA coating in NaCl revealing air trapping visible as an air bubble and the associated 2D fluorescent confocal micrographs showing presence or absence of adhered bacteria on zones without or with trapped air respectively; **(B)** Surface coverage by air of coatings with Cassie-Baxter state after 3h of immersion in NaCl, M63G and LB media. (***: p-value < 0,01, **: p-value < 0,05).

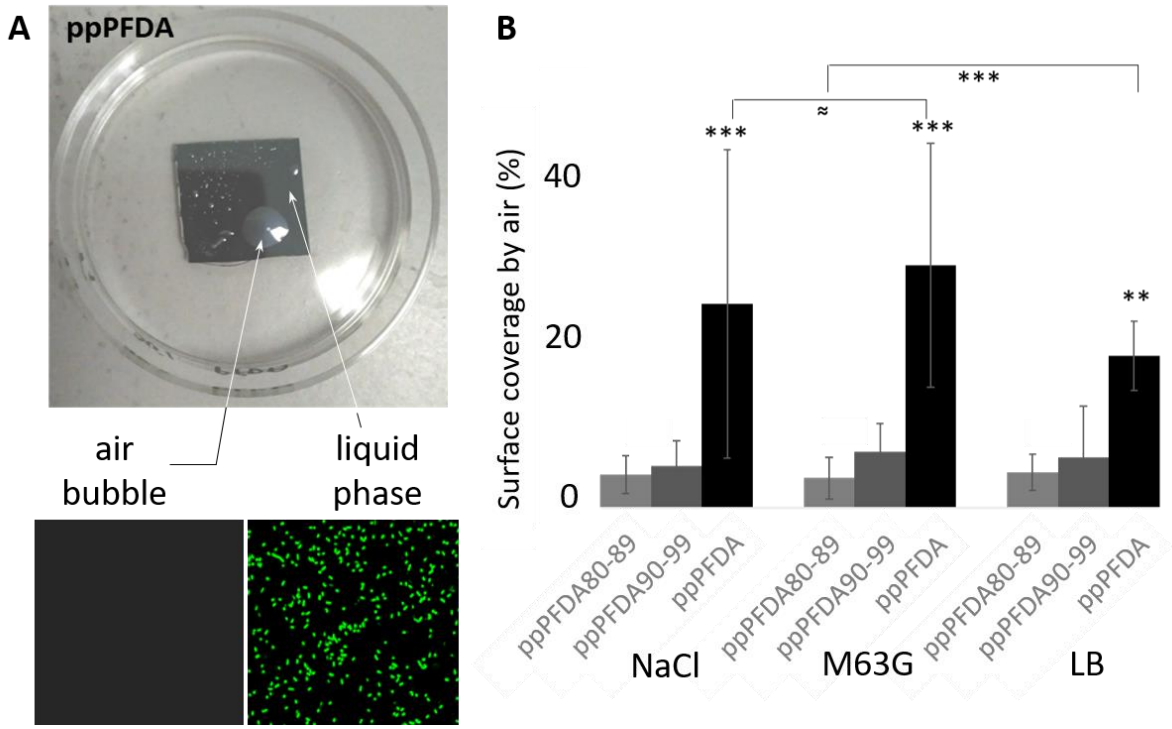

Figure S8: Number of *Staphylococcus epidermidis* bacteria adhered on coatings of different %PFDA and on SW and PP reference surfaces after 1h of culture in LB medium. ## and #: Significant difference compared to SW ($\alpha < 0.01$ and $\alpha < 0.05$); §§ and §: Significant difference compared to PP ($\alpha < 0.01$ and $\alpha < 0.05$); ** and *: Significant difference between coatings ($\alpha < 0.01$ and $\alpha < 0.05$). n: number of values for a given surface in the given conditions.

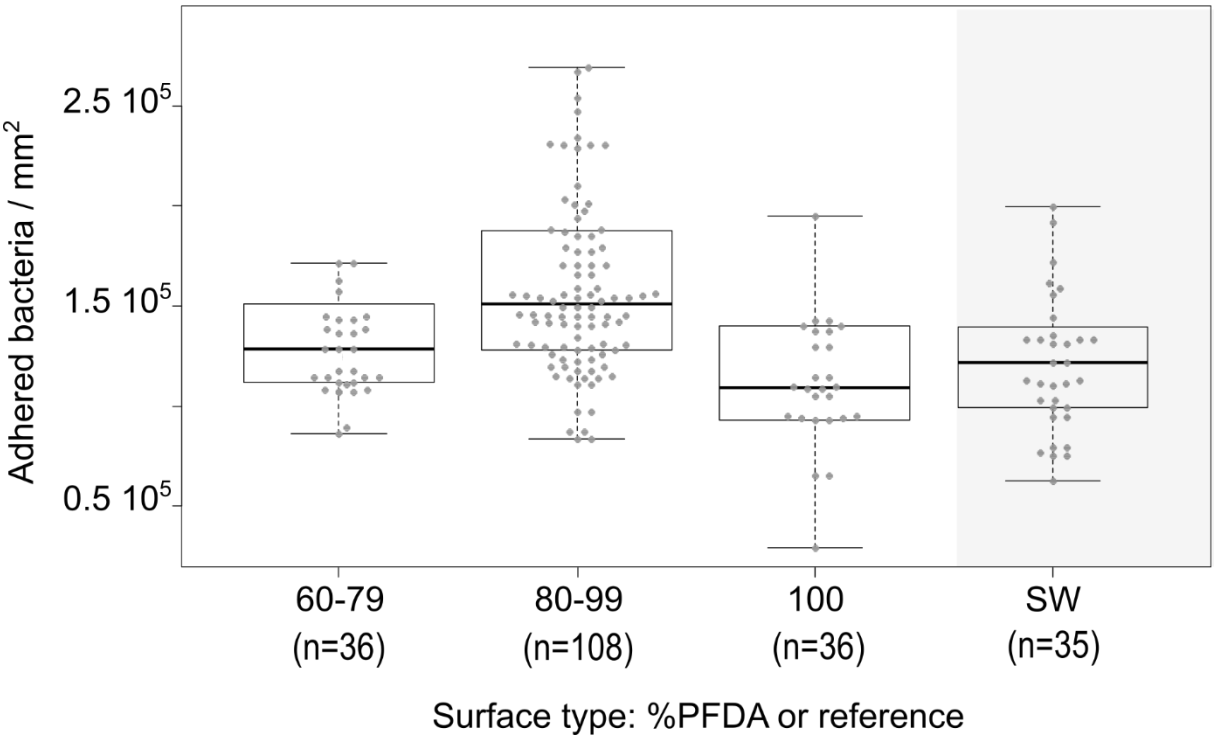

Figure S9: %PFDA as determined by XPS analysis on **(A)** ppPFDA40 and **(B)** ppPFDA100 coatings before (red line) and after 3h immersion in three different culture media (NaCl, M63G and LB)**.** After immersion, one place without visible fouling (grey) and one place with visible fouling (black) were analyzed for each coating. Measurement was done on two independent samples of %PFDA.

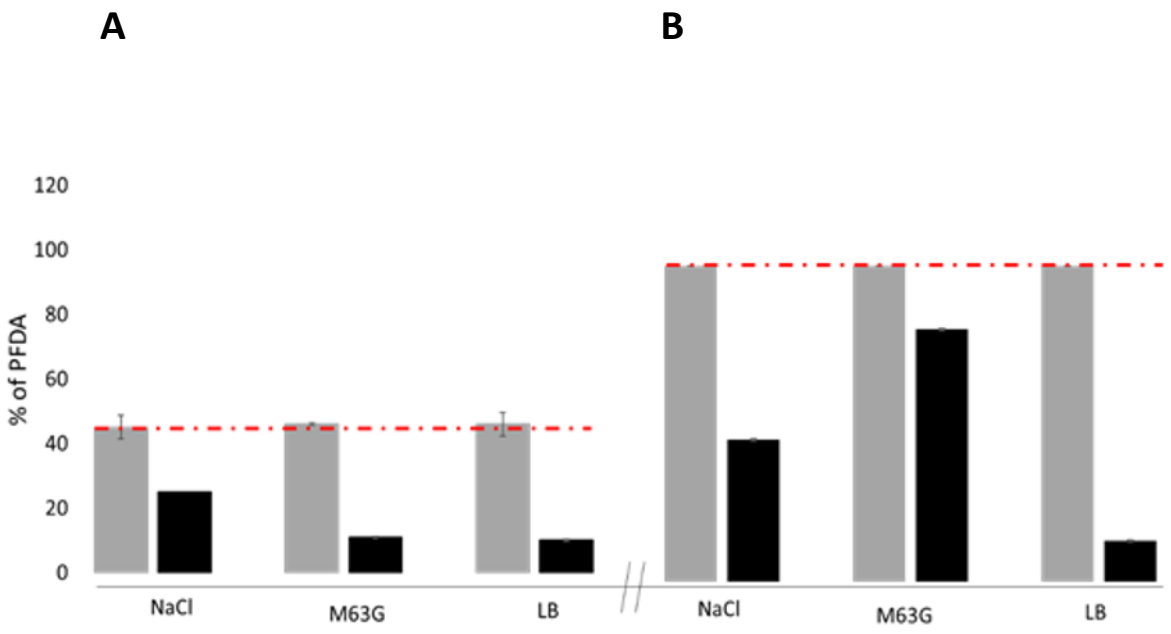

Figure S10: Calculation of %PFDA on the basis of the peak areas of each element measured on XPS high-resolution spectra. Transmission function of the spectrometer, cross section, free average course (Briggs, D., *Surface Analysis of Polymers by XPS and Static SIMS*. Cambridge University Press: Cambridge, **1998**.) and the theoretical atomic ratios in the structure of each molecule are considered. Effective cross-section is 1.00 for C (1s), 4.43 for F (1s) and 2.93 for O (1s).

$$\%PFDA = A_{F1s} + 2 \times A_{CF2} + A_{CF3}. \quad \textbf{(S4)}$$

knowing that

$$\%PFDA = \%F_{PFDA} + \%O_{PFDA} + \%C_{PFDA} \quad \textbf{(S5)}$$

and

$$\%F_{PFDA} = A_{F1s}, \quad \textbf{(S6)}$$

$$\%O_{PFDA} = \frac{A_{CF2}}{7} \times 2, \quad \textbf{(S7)}$$

$$\%C_{PFDA} = \%[CF3] + \%[CF2] + \%[C-C]_{PFDA} + \%[C=O, C-O]_{PFDA}, \quad \textbf{(S8)}$$

with

$$\%[CF3] = A_{CF3}, \quad \textbf{(S9)}$$

$$\%[CF2] = A_{CF2}, \quad \textbf{(S10)}$$

$$\%[C-C]_{PFDA} = \frac{A_{CF2}}{7} \times 3, \quad \textbf{(S11)}$$

$$\%[C=O, -C-O]_{PFDA} = \frac{A_{CF2}}{7} \times 2. \quad \textbf{(S12)}$$